

CSA GROUP™

STANDARDS RESEARCH

Dynamic Load Allowance for Bridges Subject to Autonomous Truck Platoons

November 2024

Authors

Sikandar Hayat Sajid, Ph.D., McGill University

Luc Chouinard, Professor, McGill University

Project Advisory Panel

Alex Au, Ontario Ministry of Transportation

Darrel Gagnon, COWI North America Ltd.

Frédéric Legeron, Parsons Corporation

Majid-Reza Irfani, Ministère des Transports, de la Mobilité durable et de l'Électrification des transports

Matthew Sjaarda, WSP Canada

Rocío Morales Rayas, CSA Group

Mark Braiter, CSA Group (Project Manager)

Disclaimer

This work has been produced by the author and is owned by Canadian Standards Association. It is designed to provide general information in regard to the subject matter covered. The views expressed in this publication are those of the author and interviewees. The author and Canadian Standards Association are not responsible for any loss or damage which might occur as a result of your reliance or use of the content in this publication.

Table of Contents

Executive Summary 4

1 Introduction 5

2 Literature Review on Autonomous Truck Platooning 6

2.1 Dynamic Load Allowance Provisions by Current Design Guidelines 7

3 Finite Element Modelling 9

3.1 Truck Load Modelling 9

3.1.1 Selection of Candidate Truck 9

3.1.2 Modelling of Truck Loads 12

3.2 Road Surface Roughness Modelling 13

3.2.1 Generating Road Surface Roughness Profiles 13

3.2.2 Implementation of Road Surface Roughness Profiles in Finite Element Tool 17

3.3 Numerical Simulations 18

4 Results and Discussion 21

4.1 Effect of Speed and Inter-Truck Spacing 22

4.2 Effect of Pavement Surface Roughness 27

5 Concluding Remarks 29

6 Recommendations for Future Work 29

References 30

Executive Summary

This report presents the results from a research project on the dynamic load allowance (DLA) for bridges subjected to autonomous truck platoons (ATPs). A brief overview of the project is presented followed by a comprehensive literature review on platooning configurations and their effect on bridges, the selection of candidate trucks to constitute an ATP, and DLA analyses. Next, the modelling of trucks, the road surface roughness generation in MATLAB, and its realization in Abaqus as 3D finite element modelling are presented in detail.

A comprehensive investigation was performed to identify the candidate truck using weigh-in-motion datasets published in the literature. Based on this review, the Federal Highway Administration (FHWA) Class 9 truck with five axles was selected for the platoons. A parametric study of the DLA was performed for a single span steel girder bridge for a single truck and for platoons with two or three trucks, with speeds ranging from 60 to 100 km/h, inter-truck spacings between 6 m to 10 m, and three road surface roughness profiles (ISO 8608 profile A, ISO 8608 profile B, and ISO 8608 profile C).

The results indicate that the resonance of the bridge can be excited by truck platoons for specific speed and inter-truck spacings, which can increase the DLA relative to that of a single truck. Combinations of platoon speed and spacing that result in resonance conditions and high DLA vary as a function of surface roughness. When resonance conditions are not encountered and inter-truck spacings are small, such that all platoon trucks are simultaneously on the span, the DLA is smaller compared to a single truck for smooth surface profiles. Large inter-truck spacings for 2-truck and 3-truck platoons result in high DLA but lower static loads, which can result in dynamic effects that are not within the current CSA S6, *Canadian Highway Bridge Design Code* guidelines, particularly for greater road surface roughness. ATPs on a smooth profile result in only marginal increases in DLA compared to a single truck and are within current CSA S6:19 guidelines.

Considering the results of the analyses conducted for this report, future work is recommended to compare the trends observed in DLA for different span lengths, bridge types, larger number of trucks, and multiple simultaneous presence effects.



"Truck platooning is largely accepted by relevant parties due to its potential to reduce greenhouse gas emissions and save fuel."

1 Introduction

Cooperative adaptive cruise control is a promising technology that allows trucks to form platoons with short inter-truck distances using wireless inter-truck communication [1]. Truck platooning is largely accepted by relevant parties due to its potential to reduce greenhouse gas emissions and save fuel. Computational fluid dynamic studies show that driving at closer inter-truck spacing considerably decreases drag forces on the trucks behind the leading truck [2] while reducing fuel consumption for the following and leading trucks [3]. The fuel savings for a 2-truck platoon can range from 7% to 28%, depending on the specific platoon parameters [3], [4]. In 2017, freight transportation accounted for 71.5% of the total United States trucking industry. The use of truck platooning could therefore lead to substantial economic and environmental benefits [5]. Furthermore, the close spacing between trucks in platooning helps to decrease the occurrence of traffic congestion [6] and enhances traffic throughput [7]. However, the deployment of platoons on highways has raised several concerns, including the negative impact on visibility of signage [8], lateral traffic safety [9], and an increase in pavement distress [10]. It has also been reported that introducing truck platooning at closer spacing poses a potential risk of structural inadequacy for bridges with lower rating factors [11].

The trucking industry has yet to formulate and implement sophisticated fleet planning and platoon operations necessary for the full realization of benefits from autonomous truck platoons (ATPs) [1]. Apart from operational issues, research is needed to determine the suitability of existing infrastructure, such as bridges, to accommodate loads of ATPs. This is crucial to provide comprehensive guidelines for the implementation of platooning technology in the transportation system.

Sajid *et al.* investigated the influence of live loads from ATPs on the reliability of bridges designed according to existing bridge design guidelines, such as the American Association of State Highway and Transportation Officials (AASHTO) load factor design (LFD) and load and resistance factor design (LRFD) specifications [12]. The study showed that the dynamic amplification factor, or dynamic load allowance (DLA), currently given by the AASHTO LRFD *Bridge Design Specifications* [13] may be conservative for ATPs. The research conducted for this report had similar objectives specific to the Canadian context and the potential impact on the relevant provisions in CSA S6 [14]. The current consensus is that DLA is expected to be lower with an increase in the number of closely spaced trucks due to the increased static load [15], [16], [17], but this needs to be substantiated for ATPs. Specifically, this report had the following objectives:

a. Perform an in-depth literature review of the dynamic load for truck platooning;

b. Review specifications for platooning configurations and constituent trucks in the literature;

c. Develop a model (finite element model with Abaqus) for a representative bridge, and perform dynamic analysis for various platoons;

d. Perform parametric studies (span length; number, spacing, speed, and weight of trucks) to quantify the maximum mid-span deflection of the bridge for static platoon loads and for moving loads to quantify the DLA;

e. Repeat steps c and d for different road surface roughness profiles; and

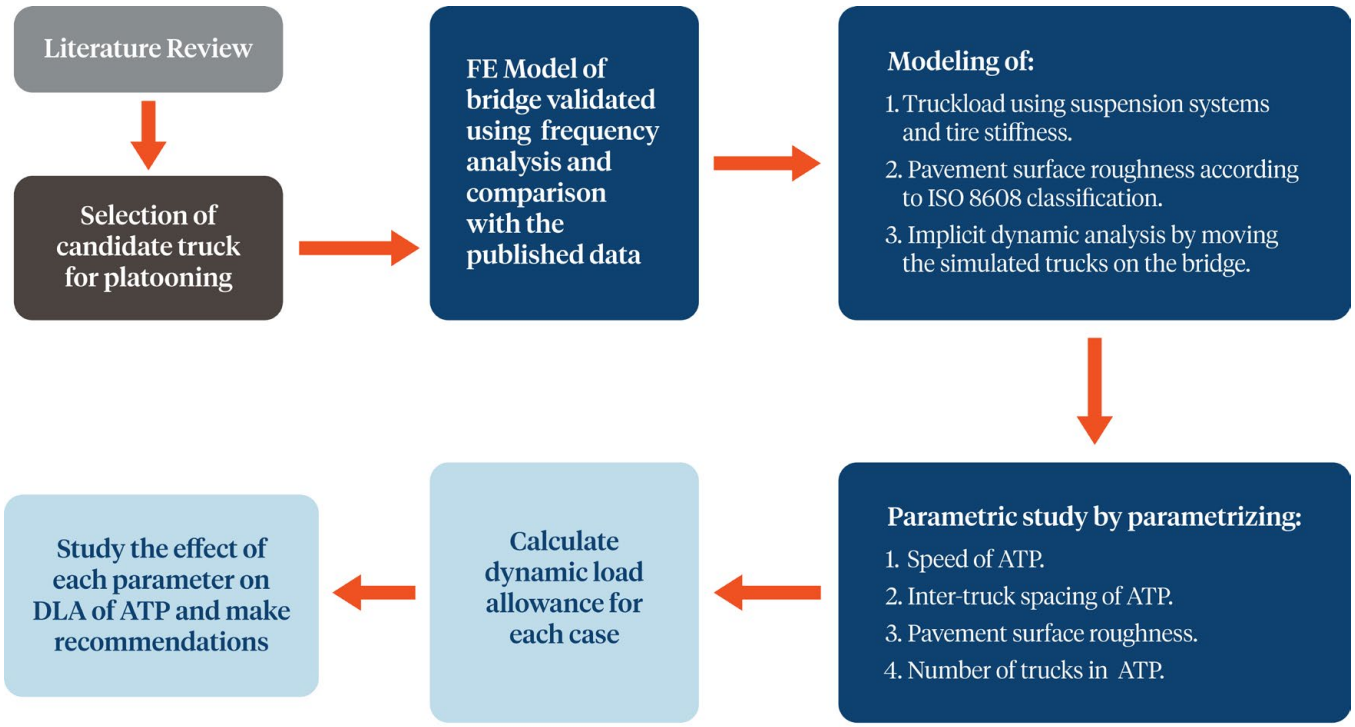
f. Perform statistical analysis of the results and propose DLA for consideration in CSA S6 along with recommendations for further studies.

The research was performed according to the schematic provided in Figure 1.

2 Literature Review on Autonomous Truck Platooning

Autonomous truck platooning has been the focus of significant research interest in the transportation industry over the past decade. In particular, frameworks and models have been proposed to quantify the influence of truck platoons on existing bridges [18]. Most of these have been parametric studies on the effect of platoons on the safety of bridges designed according to existing standards [12], [19], [20], [21]. Yarnold and Weidner [19] evaluated the shear force and bending moment from platoons of Florida Department of Transportation (FDOT) C5 standard trucks for single and continuous span bridges, as a relation of the headway distance between trucks and span length.

Figure 1: Flow chart of the sequence of research.



A comparison of results with AASHTO LRFD live loads indicated that loads on long span bridges can be a problem when closely spaced ATPs are used. These findings are consistent with those reported by Sajid *et al.* [12] and Ling *et al.* [22].

Tohme and Yarnold [20] evaluated the load rating of ATPs for a range of headway distances (6–12 m) and span lengths (32–68 m) for a benchmark steel composite concrete bridge from the AASHTO *Manual for Bridge Evaluation* [23]. The results indicated that in the positive bending moment region, allowable stress ratings may be reduced for all the platoon combinations carried out in previous studies. Likewise, the ratings may be minimized in the negative moment regions for the majority of span lengths [20]. Furthermore, the load factor ratings were acceptable for ATPs in the positive moment region and inadequate for all span lengths in the negative moment regions. Elshazli *et al.* reported results from 29,600 computer simulations by parametrizing different characteristics of platoons [24]. They determined the headway spacing and number of trucks in the platoon as the main critical parameters influencing the bridge rating [25]. Braguim *et al.* studied the possible reduction in fatigue damage for steel girder bridges that platooning might allow [21]. They performed line girder analyses on simple and continuos span bridges for arrays of truck platoons, and used rainflow counting to determine number of cycles and stress range. Subsequently, they quantified the fatigue damage using the Miner's rule. AASHTO LRFD fatigue loads were used to normalize the fatigue damage for diverse platoon arrays. Although platooning magnified the load effects, the consistent truck movement decreased the stress cycles, which helped to reduce fatigue damage in some instances. Thulaseedharan and Yarnold studied the deployment of ATPs prioritizing prestressed concrete bridges in Texas [26]. They used the National Bridge Inventory load and structural condition ratings for truck platoons to prioritize bridges for detailed assessment before authorization for truck platooning. Wassef [27] performed a detailed study to identify potential trucks for platooning configurations. This study included most of the trucks used in previous studies, except the FDOT C5 truck. Yang *et al.* studied the influence of variability of headway spacing, platoon load, span length, and load amplification factor on the safety of certain bridges that were simple and two-span continuous, with span lengths varying from 9.14 to 61 m, and were planned according to the AASHTO LRFD bridge design provisions [28]. However, this study did not consider live load effects, such as the dynamic amplification and bias factors. In addition, the bridges included in the study were only designed using the AASHTO LRFD provisions.

In a sensitivity study for the reliability analysis of a steel composite bridge, Sajid *et al.* determined the safe deployment of ATPs relative to both AASHTO LRFD and LFD bridge design guidelines on current bridges [12]. They calculated reliability indices for steel composite bridges that followed both AASHTO guidelines for diverse settings of ATP live loads by parameterizing the variability, bias, and dynamic amplification [12]. These factors were not taken into account by Steelman *et al.* [29], but were introduced by Sajid *et al.* [12], who noted that the reliability could be significantly influenced by the DLA factor currently stipulated in the AASHTO LRFD *Bridge Design Specifications* [13].

In general, the current literature on autonomous truck platooning indicates that a higher number of trucks on a bridge decreases the DLA due to a higher total static load. CSA S6 provisions describe the DLA in terms of an equivalent static load, which is a portion of the CL-W load, suggesting that increasing the number of trucks will reduce the DLA on the bridge [14]. However, Ling *et al.* reported that platooning trucks can excite resonant frequencies of some bridges, which results in an increase in DLA above the levels specified in the Chinese, European, and AASHTO LRFD codes [30]. In a later study, Ling *et al.* proposed an increase in DLA factors for small- and medium-span concrete bridges in the Chinese code based on the results obtained for 4-truck platoons [31].

2.1 Dynamic Load Allowance Provisions by Current Design Guidelines

Different bridge design guidelines provide dynamic amplification factors either as a constant value, as a bridge span length, as a function of span length and bridge deck thickness, or as a function of fundamental frequency. For design purposes, the DLA depends on the axle number and is applied to a CL-W truck, an ideal 5-axle truck used in CSA S6. CSA S6 suggests the use of

component level DLA factors, as provided in Table 1. In the CSA S6 commentary, the dynamic amplification is partially dependent on the fundamental frequency, as shown in Figure 2. The corresponding fundamental frequency (f_0) can be calculated for a given span length (L) of a bridge using Equation 1, given by [32] and [33].

$$f_0 = 82L_{max}^{-0.9} \quad (1)$$

In AASHTO's 2002 *Standard Specifications for Highway Bridges,* Equation 2 is used to calculate the dynamic amplification factor (I), in which (L) is the span length (in feet) [34].

$$I = \frac{50}{L+125} \leq 0.3 \quad (2)$$

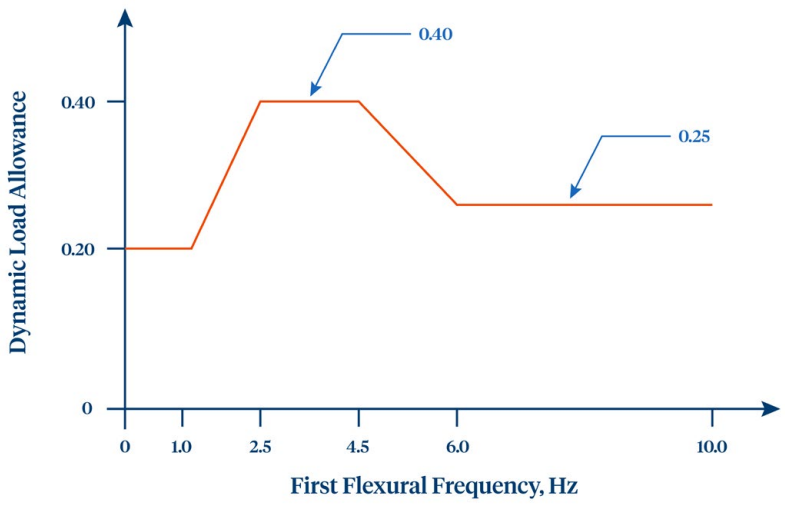
The AASHTO LRFD *Bridge Design Specifications* use a constant value of 0.33 as the dynamic amplification factor for the design truck. They also specify that the DLA at desk joints for all limit states is 75%. For all other components for fracture and fatigue limit states, the DLA is 15%, and for all other limit states, it is 33% [13]. BS 5400-2 also use a constant DLA (known as impact factor) of 25% [55].

The Eurocode uses a dynamic amplification factor (DAF), based on either shear force or bending moment. The DAF, which is a function of the number of lanes and span length, is included in the load values specified in EN 1991-2, *Eurocode 1. Actions on Structures, Part 2: Traffic Loads on Bridges* [35].

Table 1: Dynamic load allowance for components other than buried structure. Data adapted from [14].

S. No	Component	Dynamic Load Allowance
1	Deck joints	0.5
2	Spans where only one axle of the CL-W truck is used (except for deck joints)	0.4
3	Spans where any two axles of the CL-W truck, or axles 1 to 3, are used	0.3
4	Spans where three axles of the CL-W Truck, except axles 1 to 3, or more than three axles, are used	0.25

Figure 2: Dynamic load allowance as a function of frequency (reproduced from [14]).



For single lane bridges, the DAF is given by Equation 3 and Equation 4 for bending moment and shear, and for a two-lane bridge, the DAF for both bending moment and shear is given by Equation 5. For a four-lane bridge, a DAF of 1.1 is recommended.

$$DAF_{bending\ moment} = \begin{cases} 1.7 & L \leq 5m \\ 1.85 - 0.03\mathrm{L} & 5\mathrm{m} < L < 15\mathrm{m} \\ 1.4 & L \geq 15m \end{cases} \quad (3)$$

$$DAF_{shear\ force} = \begin{cases} 1.4 & L \leq 5m \\ 1.45 - 0.01\mathrm{L} & 5\mathrm{m} < L < 25\mathrm{m} \\ 1.2 & L \geq 25m \end{cases} \quad (4)$$

$$DAF = \begin{cases} 1.3 - \frac{0.4}{100}L & L \leq 50m \\ 1.1 & L > 50m \end{cases} \quad (5)$$

Currently, the British Standard and CHBDC S6 uses a DLA of 1.25 compared to AASHTO LRFD that uses 1.33. A more detailed review of the national code provisions for the DLA of different jurisdictions is provided in [36]. However, the review does not address platooning trucks moving synchronously on a bridge.

3 Finite Element Modelling

The finite element analysis software, Abaqus, was used to model a steel girder bridge similar to the one analyzed in [16]. The general purpose linear brick element C3D8R was selected, and the mesh size was optimized with convergence analysis. The steel girders were connected to the concrete slabs using tie constraints. The bridge had five 36.6 m long W40 x 264 girders spaced at 1.625 m (on centre) that were simply supported on both ends, with diaphragms every 9.144 m. The girders supported a 177.8 mm thick by 8.128 m wide bridge slab. Grade 60 steel was used for the girders and 55.16 MPa concrete for the slab. The girders were tied to the slab to simulate the composite action of the slab and girders. Figure 3 shows the bridge model along with the mode shapes. As shown in Table 2, the mode shapes and resonance frequencies were in close agreement with those given in [16]. The dynamic analysis of the bridge was performed by considering the vehicle-bridge interactions and road surface roughness. The methodologies adopted for modelling both are explained in sections 3.1 and 3.2. It should be noted that this bridge was selected for demonstration purposes and a bridge with different characteristics will provide different results.

3.1 Truck Load Modelling

3.1.1 Selection of Candidate Truck

Selection of the candidate truck for the platooning was informed by the literature review. The most commonly used truck in the studies reviewed for this report was the Federal Highway Administration (FHWA) Class 9 truck, which is a 5-axle truck. Wassef [27] analyzed the weigh-in-motion datasets for different FHWA trucks in a variety of states across the United States. As shown in both Figure 4 and Table 3, Class 9 trucks represented the greatest percentage of FHWA trucks in Wassef's study [27]. This was also reported in other studies, such as [37]. Other researchers have used different trucks in their platooning studies, and some of these studies are listed in Table 4, along with the types of trucks each used. The literature indicated that the FHWA Class 9 truck is a suitable option to serve as a candidate truck in homogenous ATPs, and therefore it was selected as the model for this research.

Table 2: Comparison of resonance frequencies of the model and the bridge. Data adapted from [16].

Modes	Frequency		Percent Difference
	Model	Reference	
1st bending mode	1.90	2.12	-11.58
1st torsional mode	2.90	3.17	-9.31
2nd torsional mode	8.20	9.09	-10.85

Figure 3: Finite element model and the first few mode shapes of the selected bridge model.

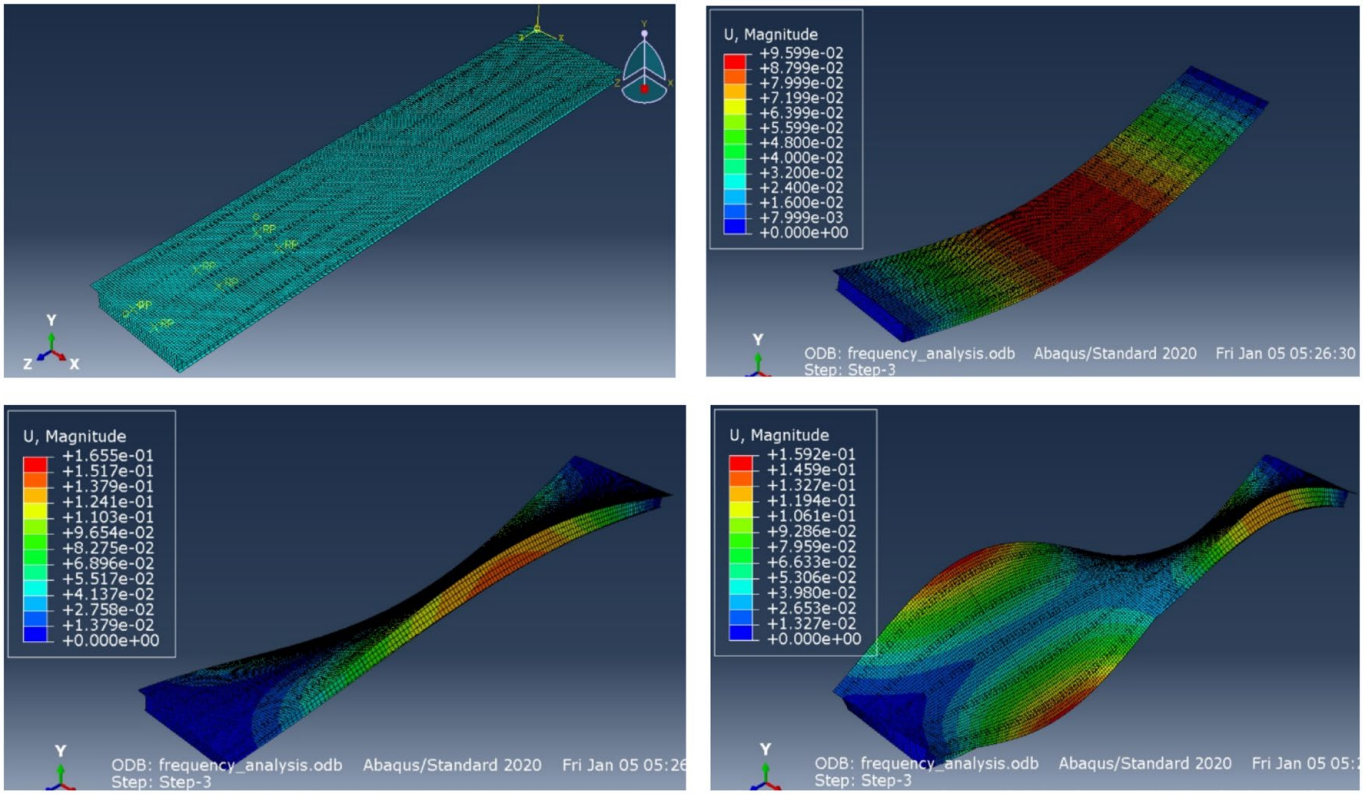


Table 3: Percentage of vehicles (GVW ≥ 20 kips) in each class based on scheme F classification. Data adapted from [27]. GVW: gross vehicle weight.

FHWA Class	Frequency									
	AL 2006-2014	AR 2008	CA 2008	DE 2008	FL 2005	ME 2008	MD 2008- 2009	PA 2008	MS 2008	VA 2008
4	2.46	0.75	1.15	7.85	1.25	1.16	1.74	0.83	3.62	0.86
5	2.20	2.76	0.15	17.36	10.84	8.72	32.56	2.73	10.81	10.75
6	3.59	1.23	10.04	10.71	4.17	4.43	7.33	1.83	3.78	6.65
7	0.58	0.07	0.17	2.42	0.47	0.14	1.28	2.72	0.04	0.37
8	3.91	1.65	3.08	3.83	3.58	4.53	7.84	1.46	5.44	5.36
9	82.80	85.29	69.29	56.88	74.77	60.87	48.67	82.68	69.56	70.45
10	1.65	0.45	0.89	0.66	0.71	19.47	0.38	0.59	0.88	0.56
11	2.15	5.63	4.64	0.19	3.15	0.58	0.01	5.46	4.30	4.21
12	0.51	2.04	0.56	0.04	0.95	0.04	0.01	1.63	1.47	0.68
13	0.15	0.12	0.15	0.05	0.12	0.08	0.18	0.07	0.09	0.10

Figure 4: Percentage of vehicles for different FHWA classes having gross vehicle weights greater than 20 kips or 88.9 kN for different states in the United States in a particular year. Figure created using the dataset provided in [27].

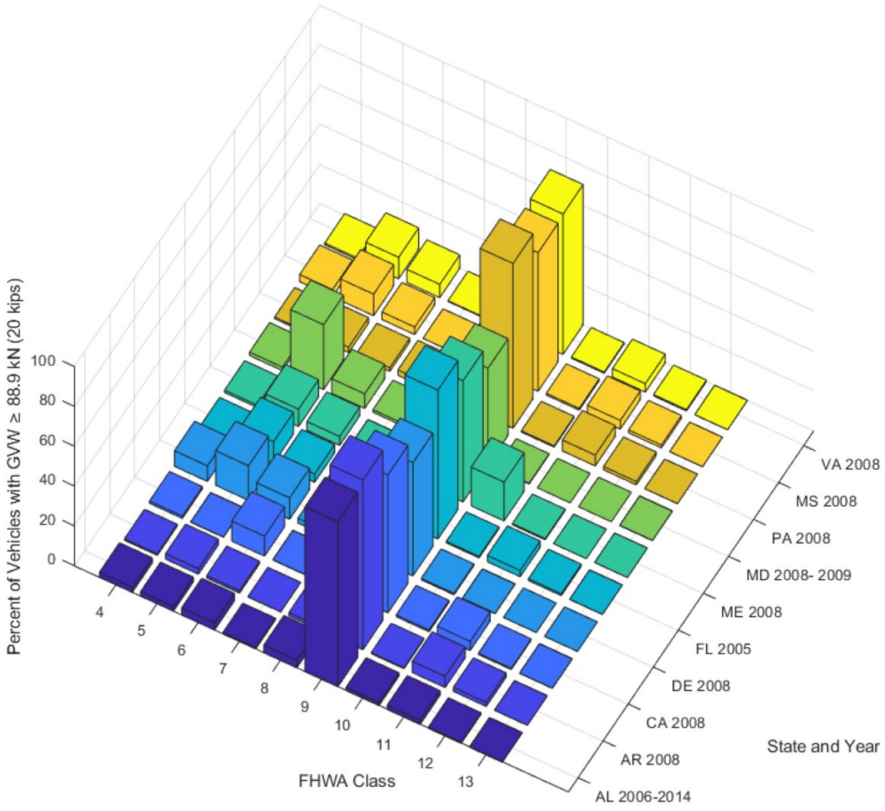


Table 4: Trucks used to constitute platoons in various published studies.

Authors	Main Premise of Research	Truck(s)	Reference
Sajid *et al.*	Reliability analysis of steel composite bridges subjected to truck platooning	FHWA Class 9 FDOT C5 NJTA Type 3S2	[12]
Yang *et al.* and Steelman *et al.*	Effects of truck platooning on girder bridges	FHWA Class 9 Type 3-3 NJTA Type 3S2 Notional rating load	[28], [29]
Yarnold and Weidner	Static load effects of truck platooning on steel girder bridges	FDOT C5	[19]
Tohme and Yarnold	Load rating of steel girder bridges owing to truck platooning	FDOT C5	[20]
Ling *et al.*	Dynamic impact of platooning loads on bridges subjected to truck platoons	FDOT C5 Chinese 5-axle truck European 5-axle truck	[30]

3.1.2 Modelling of Truck Loads

Truck loads can be modelled as simple point masses to full 3D finite element models of trucks, which are typically used to analyze loads in impact (crash) studies. Published studies have suggested several techniques to model truck loads. The point mass approach was used in [16] to model vehicle-bridge interaction for calculating the dynamic amplification factor of long span bridges. In the point mass approach, the axle weights are modelled on the bridge deck and then moved across to simulate the rolling wheels of a truck. A detailed wheel point mass model has seven degrees of freedom: roll, pitch, horizontal and vertical displacement, lateral displacement, wheel spin, and yaw. In the DLA studies that used the point mass approach, only the vertical degree of freedom is considered because it is the most important parameter [16], [30]. The point mass approach includes a sprung-mass model to represent the stiffness of the truck suspension [38]. Chang *et al.* proposed a a rigid-disk model that imitates a wheel, neglecting the tire deformations, connected to the springs on the top [39]. The disk model was proposed because of the shortcomings of the point model on a rough surface. The rough surface of the pavement is a track of a series of hills and valleys and the point mass may not touch the valley points. The study reported that for displacement time history, the use of the point model to model the wheel and the disk does not result in a significant difference. However, if velocity or acceleration responses are required, then a disk model should be used as it results in lower amplitudes [39]. Ben Afia *et al.* [40] used dual spring systems to model the suspension systems and the tires, an approach that considers the stiffness of both the truck suspension system and the tires. Ling *et al.* [30] used a more detailed approach in modelling the truck loads. They incorporated the rolling and pitching moments in addition to the truck suspension system and the tire damping stiffness parameters. Furthermore, instead of using a point to apply wheel loads, they applied points on a patch equal to the width of the tire. While this is potentially a more realistic approach, the quantification of the parameters for each of these unknowns can be subjective, which may lead to unrealistic outcomes.

The research conducted for this report used a dual system, specifying both tire stiffness and damping and the truck suspension system. This model imitates the quarter car model, which has been applied in the literature for similar problems [40], [41]. The axle orientation and loading of the FHWA Class 9 truck are given in Figure 5 and Table 5, respectively. Similarly, the parameters adopted to characterize the tires and the suspension system are given in Table 6, in consideration of [31]. It should be noted that these parameters are not invariantly available in the literature, and therefore a more rational approach for normalization or referencing of final results should be used to minimize the uncertainty associated with these values.

Figure 5: Axle topology of FHWA Class 9 truck.

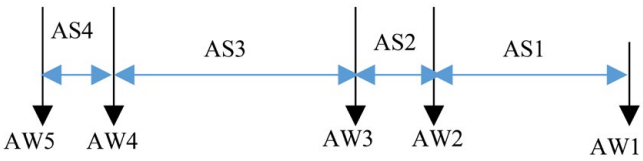


Table 5: Axle spacing and axle loads of FHWA Class 9 Truck corresponding to Figure 5. The total truck weight is 355.4 kN.

Truck	Total Length (m)	AS1 (m)	AS2 (m)	AS3 (m)	AS4 (m)	AW1 (kN)	AW2 (kN)	AW3 (kN)	AW4 (kN)	AW5 (kN)
FHWA Class 9	15.54	3.66	1.22	9.45	1.22	53.4	75.6	75.6	75.6	75.6

Table 6: Values adopted for each parameter of the FHWA Class 9 truck modeled in Abaqus

Parameter	Axle	Unit	Values
Suspension stiffness coefficient	Axle-1	N/m	300,000
	Axle-2	N/m	500,000
	Axle-3	N/m	500,000
	Axle-4	N/m	400,000
	Axle-5	N/m	400,000
Tire vertical stiffness	Axle-1	N.s/m	10,000
	Axle-2-5	N.s/m	53,000
Tire vertical stiffness	Axle-1	N/m	1,500,000
	Axle-2	N/m	3,000,000
	Axle-3	N/m	3,000,000
	Axle-4	N/m	3,000,000
Tire damping coefficient	Axle 1-5	N.s/m	2,000

3.2 Road Surface Roughness Modelling

3.2.1 Generating Road Surface Roughness Profiles

The dynamic analysis of the bridge was performed by considering the vehicle-bridge interactions and road surface roughness. Several approaches can be used for the simulation of road surface roughness, and the most common are based on either a shaping filter or a sinusoidal approximation [42], [43]. The shaping filter approach applies a filter to a white noise signal to reproduce specified statistical properties of the road surface. The sinusoidal approach uses a power spectral density (PSD) function [44] to generate random pavement surface profiles in agreement with the ISO 8608 classification [45].

Road surface roughness follows a standardized classification system, as described in ISO 8608, *Mechanical Vibration — Road Surface Profiles — Reporting of Measured Data* [46]. This classification ranges from A to H, where A indicates a smooth road surface and H refers to a road surface that can only allow crawling speeds. These roughness profiles are a function of the lower and upper limits of PSD of vertical displacement and PSD of acceleration. The concepts in ISO 8608 are road profile, spatial frequency, and PSD. Spatial frequency is defined in cycles/m. Road profile is the changes in the height of the road surface measured along a track and parallel to the road. The ISO 8608 roughness co-efficient, $G_d\,(n_0)$, for each class of profile is provided in Table 7.

Table 7: ISO 8608 Classification relative to roughness coefficient values. Data adapted from [45]. n_0 = 0.1 cycles/m.

Road Class	$G_d\,(n_0)(10^{-6}m^3)$	
	Lower limit	Upper limit
A	—	32
B	32	128
C	128	512
D	512	2048
E	2048	8192
F	8192	32768
G	32768	131072
H	131072	—



"The dynamic analysis of the bridge was performed by considering the vehicle-bridge interactions and road surface roughness."

A comparison of different profiles for various roughness classes is provided in Figure 6. The profile generated a random phase angle and a distribution of heights along the longitudinal axis of the bridge. The effect of the random phase angle is shown in Figure 7 for a single class of surface roughness for a given ISO 8608 profile A-B. It should be noted that the random phase angle resulted in random locations for the "hills" and "valleys" in the profile. The pavement surface roughness profiles were generated using a MATLAB code, in consideration of [45]. The actual profiles of road surface roughness are classified according to the International Roughness Index [47], which was developed by the World Bank and is used in code calibration efforts, such as [15]. In one study, artificial profiles generated according to the ISO 8608 classification were compared to actual profiles observed in the field using the International Roughness Index [48]. The study's sensitivity analysis for different parameters of the artificial profiles showed that care should be taken when selecting the inputs to these parameters. For this report, the effect of the sampling interval was studied and it was concluded that using a very small sampling interval (i.e., 0.01 m) to create the surface roughness profile may not be practical. After some sensitivity analysis, a sampling interval of 100 mm was selected, which is consistent with similar studies [49]. This approach for artificial road surface roughness profile generation is also consistent with various published studies [30], [31], [40], [45]. In the research conducted for this report, three road surface roughness profiles were generated using MATLAB for ISO 8608 profiles A, B, and C, using lower limits of roughness coefficient values for the respective profiles, as provided in Table 7 and shown in Figure 8.

The literature also provided other simplified approaches for the realization of road surface roughness in the finite element code. One example is modelling the surface roughness as the total interacting force on the bridge, which is the sum of the weight of the truck and the variation in the vertical interacting force due to road surface roughness, the wheel hop, and the associated body bounce vibrations [16]. The wheel hop is due to the bump at the bridge entrance, which produces an impact that results in vibrations in the range of 16 Hz from the wheels, independent of the truck body [50]. In [16], the vertical interacting force was taken as 10% of the weight of an HS-20 truck, and the resulting vertical interacting force was generated using a sinusoidal function, as shown in Figure 9 for a rear axle weight of 8 tons (16 kips) and 10% variation. This example was implemented in Abaqus for the composite bridge shown in Figure 3, which resulted in a DLA of 9% for an HS-20 truck with a speed of 65 km/h compared to the crawling speed, as shown in Equation 6.

$$DLA = \left(1 - \frac{Max(Deflection)_{65\ km/hr}}{Max(Deflection)_{crawling\ speed}}\right) x\ 100\% = \left(1 - \frac{12.92mm}{11.79}\right) x\ 100\% = 9\% \quad (6)$$

Figure 6: Pavement surface roughness profiles for various roughness classes.

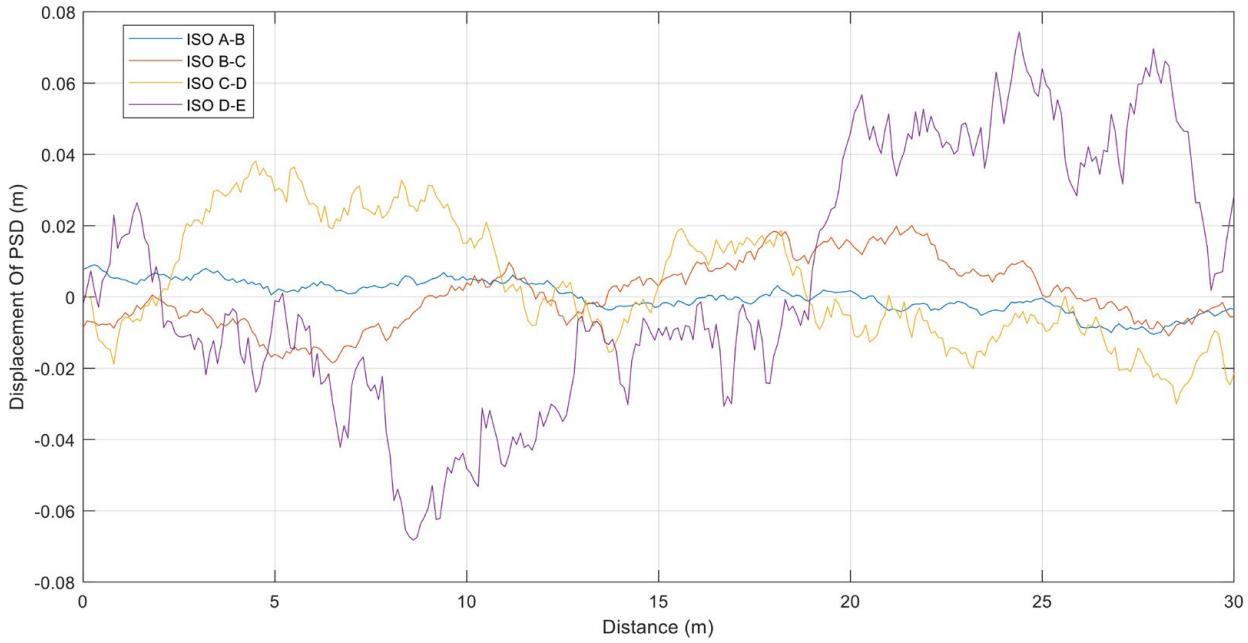


Figure 7: Effect of random phase angle on the pavement surface roughness profile.

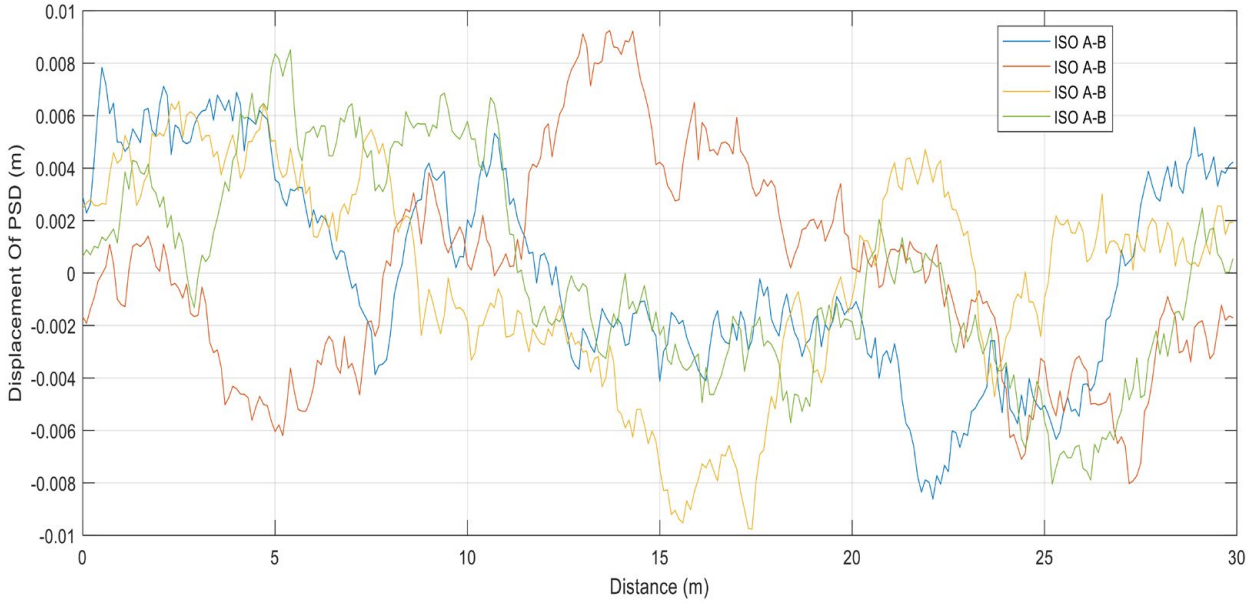


Figure 8: Road surface roughness profiles for (a) ISO 8608 profile A, (b) ISO 8608 profile B, and (c) ISO 8608 profile C.

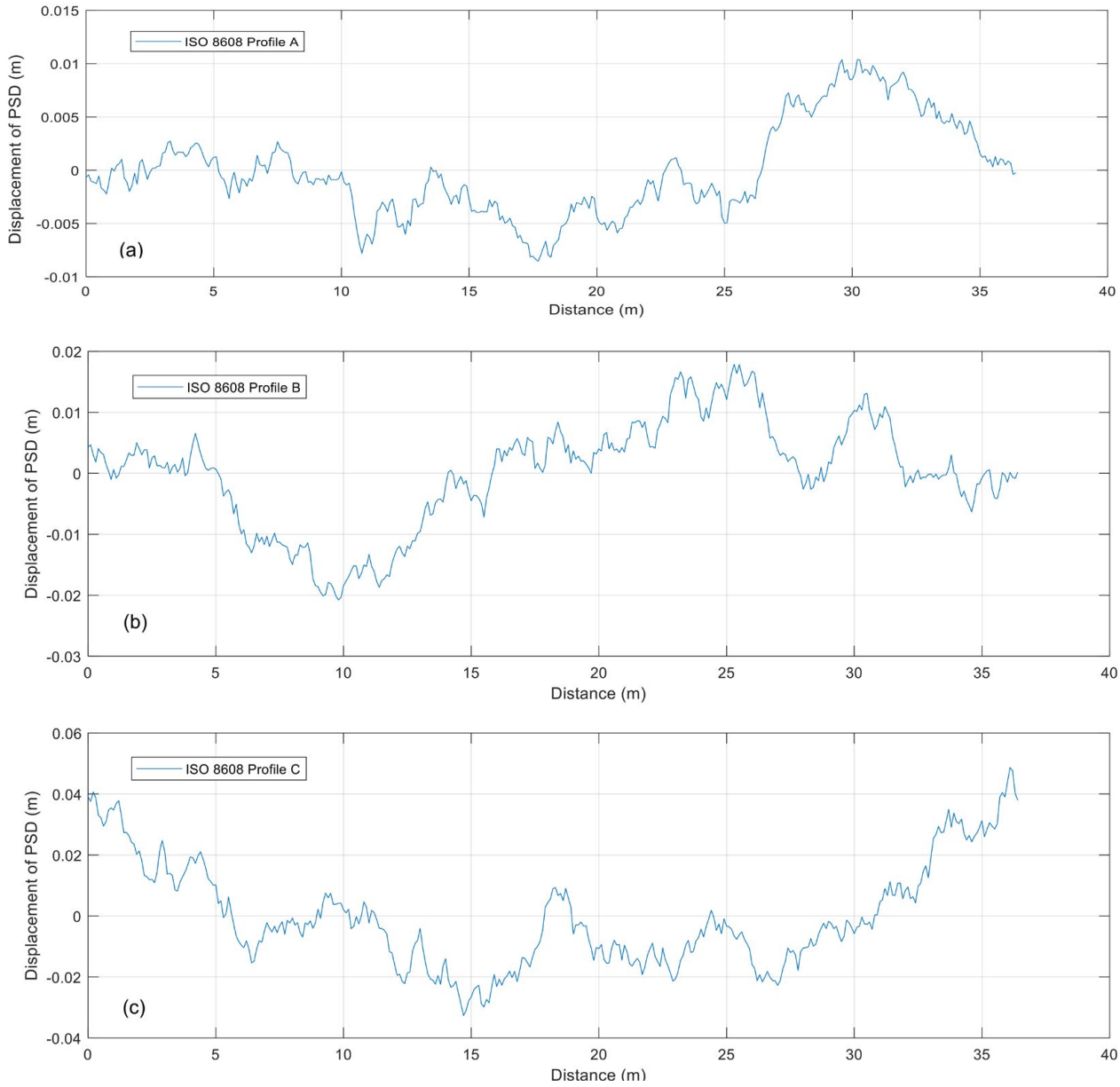
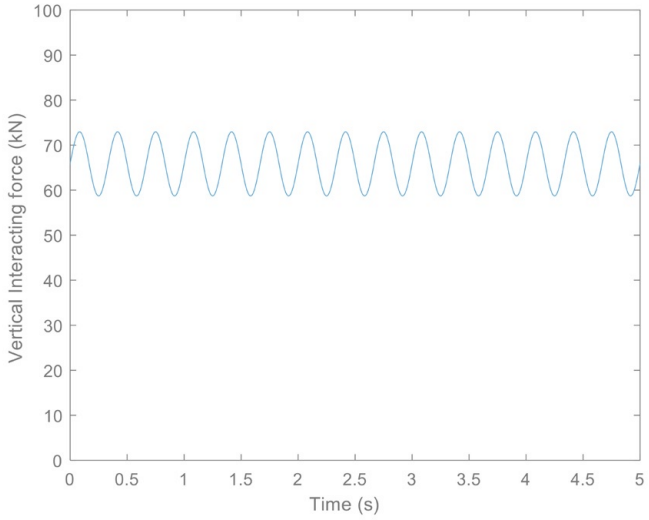


Figure 9: Vertical interaction force using sinusoid of body vibrations in the bridge due to the moving truck.



Figures 10 and 11 compare the deflection time history due to the HS-20 truck moving on the bridge at a speed of 65 km/h and at a crawling speed. The issue with this approach, however, is the lack of relationship between the variation of the vertical interacting forces and the ISO 8608 roughness profiles.

Another example is modelling the surface roughness by generating roughness profiles using a PSD approach for a particular ISO 8608 surface roughness profile and then caculating the vertical force as a PSD profile value at that instant and the stiffness of the suspension system of the passing truck, and subsequently model the vertical forces at each instant of time [40]. For multiple trucks, however, this approach can be inefficient.

3.2.2 Implementation of Road Surface Roughness Profiles in Finite Element Tool

The roughness profiles generated using MATLAB were implemented in Abaqus on the bridge deck for the parametric studies, which are discussed in Section 4. First, the generated road surface roughness profile heights for each interval of longitudinal length of bridge deck were used to generate a 3D matrix. It should be noted that the heights only change in the longitudinal direction of the bridge deck; they are constant in the lateral direction (which is the transverse of the bridge deck). This modelling strategy is consistent with a similar published study [51]. Next, the RufGen plug-in [52] for Abaqus was used to import the generated 3D profile for each case (writing a user defined subroutine for rough surface generation in Abaqus is an alternate option). The RufGen plug-in imports the surface roughness as an orphan mesh, from which a part is created using another plug-in to create geometry from mesh. The interactions are then defined to assign this part to the bridge deck to characterize the surface roughness. A close-up view of typical surface roughness defined on a bridge deck is shown in Figure 12. This was generated using the ISO 8608 profile C.

Figure 10: Deflection curve of the composite bridge modelled in section 3 under the HS-20 truck moving at a speed of 65 km/h.

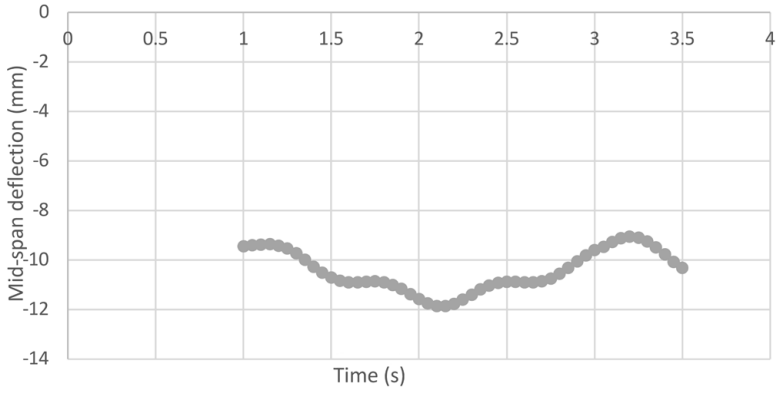
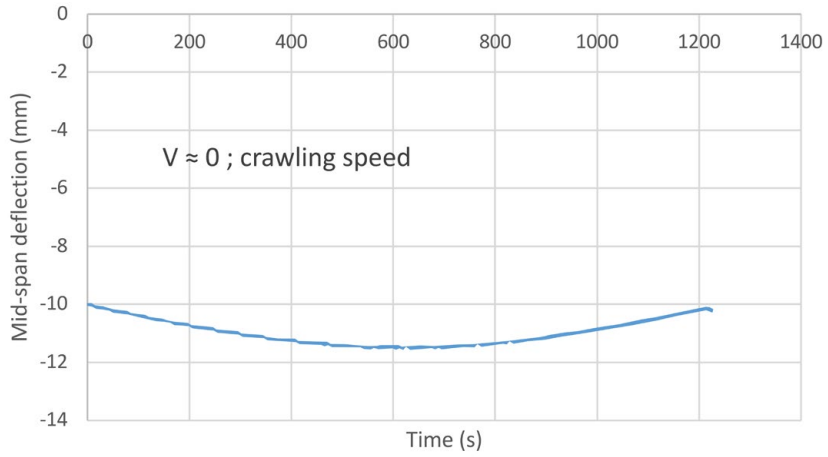


Figure 11: Deflection curve of the composite bridge modelled in section 3 under the HS-20 truck moving at a crawl.



The distribution of the surface roughness can be observed. A magnified image of the bridge mesh of the same profile C is shown in Figure 13, which provides better physical context of the road surface roughness characterization. Following the road surface roughness definition in Abaqus, the truck wheels were simulated at a given speed on the exterior lane of the bridge deck and implicit dynamic analysis was performed to obtain the deflection time history at the mid-point of the exterior girder. The exterior lane and exterior girders were selected because they undergo the highest deflection under truck loads [51].

3.3 Numerical Simulations

The methodology followed in this research report is outlined in Figure 14. The process started by developing a numerical model of a steel composite bridge in Abaqus in consideration of the literature [16]. The bridge was confirmed for its accuracy using frequency analysis in Abaqus. Subsequently, the FHWA Class 9 truck was selected to constitute different truck platoon arrangements with different inter-truck spacings and number of trucks. Inter-truck spacing was defined as "the distance between the rear axle of the front truck and the front axle of the rear truck" [16]. Platoons were then generated and driven across the bridge on the exterior lane. Each of the generated platoons were driven across the selected bridge with simulated ISO 8608 profiles A, B, and C at five different speeds: 60 km/h, 70 km/h, 80 km/h, 90 km/h, and 100 km/h. In addition, the platoons were moved at crawling speeds to calculate the DLA for each case. Given that the crawling speeds of platoons also exhibit vibration of the bridge deck, which is unrealistic, a moving average filter must be used to dampen the deflection time history. Alternatively, the centroid of the axle loads can obtained and the platoons are placed on the bridge according to that location, and then a static analysis is performed to obtain maximum deflection at mid-span on the exterior girder. The latter approach was found to be more computationally efficient and less subjective, as the former approach would require selecting the order of the filter to completely damp out the fluctuations in the deflection time history. Therefore, the latter approach was selected to obtain the maximum mid-span deflection due to static platoon. The set of simulations formed the dataset for the analysis of DLA as a function of speed, inter-truck-spacing, roughness of profiles, and number of trucks in a platoon.

The deflection time histories were generated following numerical simulations for each case outlined in Figure 14. Selected deflection time histories with different characteristic parameters are shown in Figure 15.

Figure 12: Close-up of side of exterior girder and bridge deck showing the roughness variation in the transverse and longitudinal directions of a bridge deck.

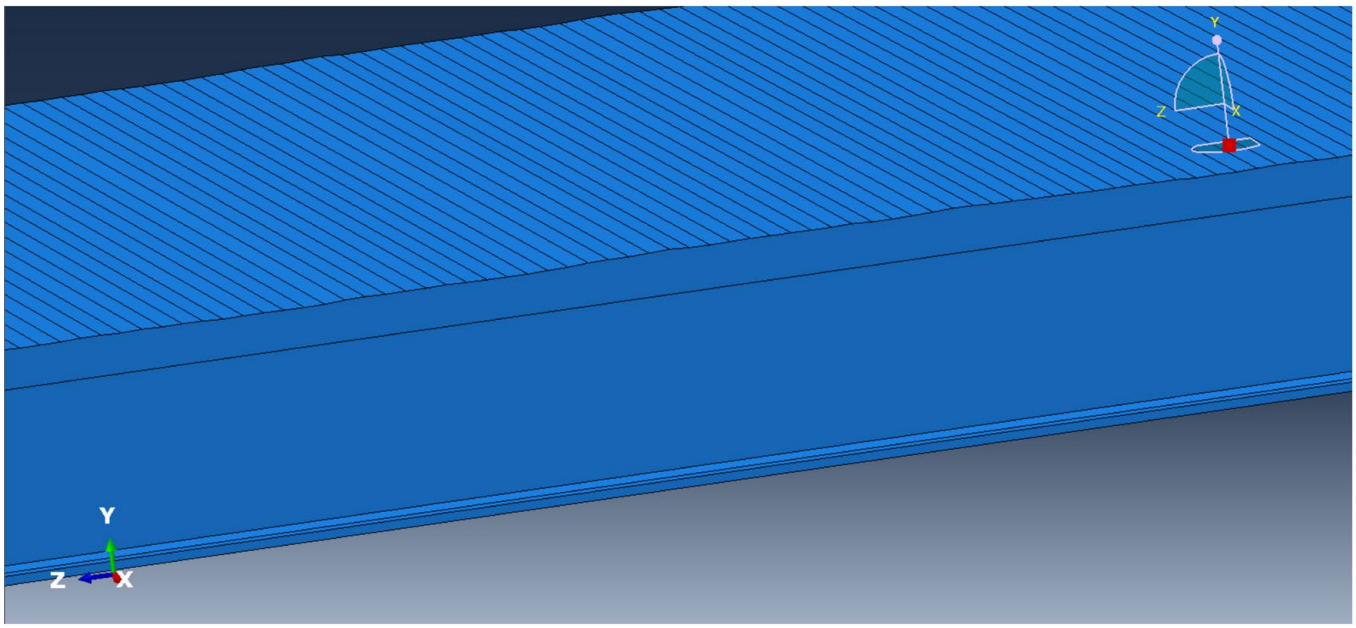


Figure 13: Close-up of bridge deck mesh showing physical surface roughness.

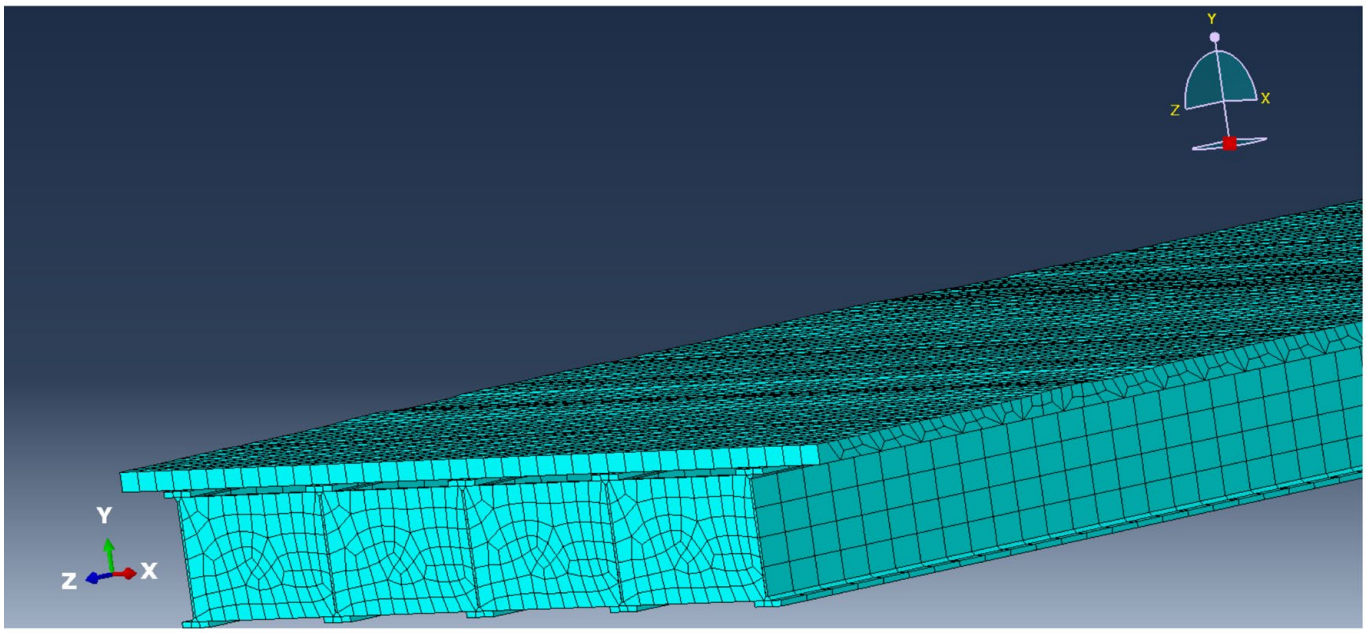


Figure 14: Flow chart of the parametric study and overall methodology for data generation.

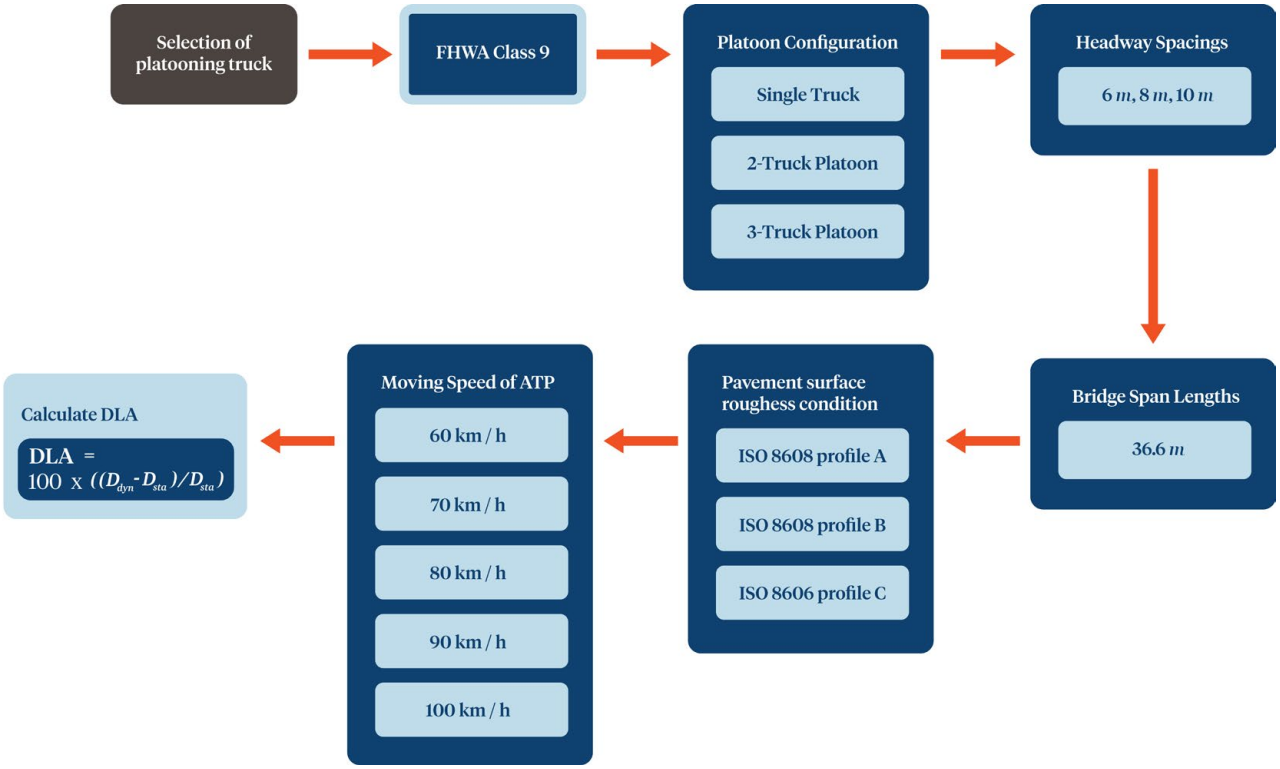
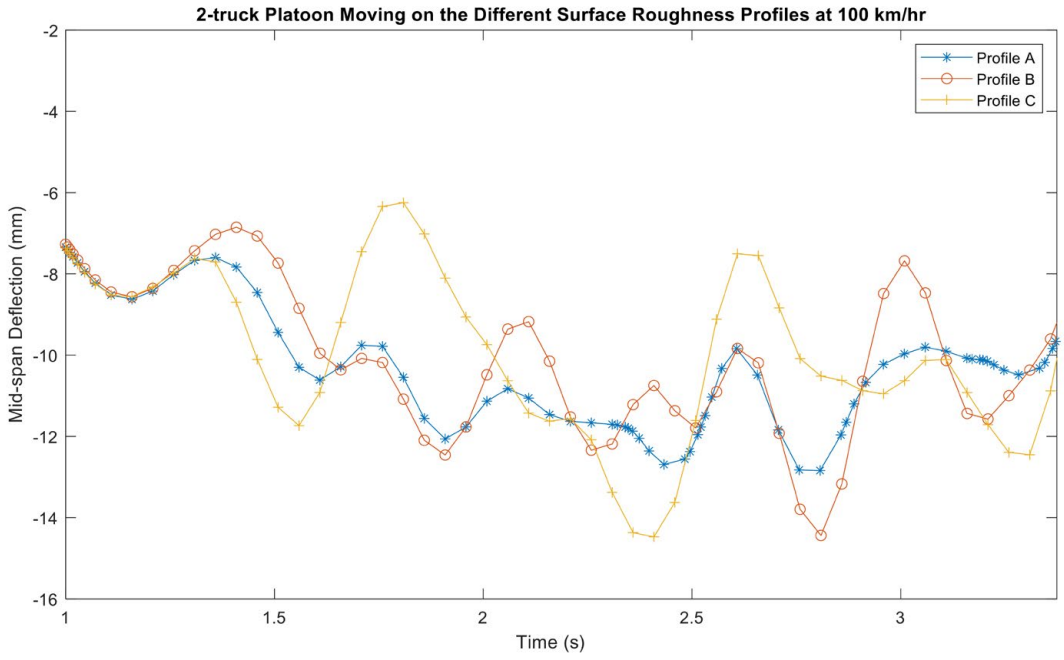


Figure 15: Deflection time histories from selected simulations comparing the effect of road surface roughness intensities characterized by ISO 8608 profiles A, B, and C.



4 Results and Discussion

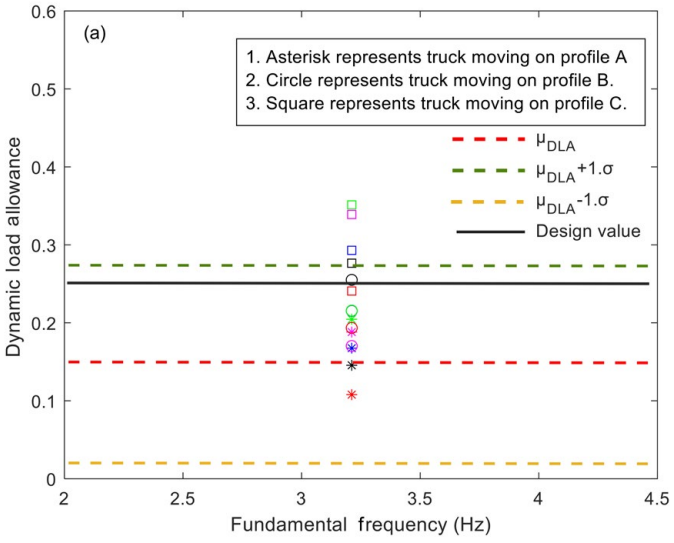
Parametric analyses were performed to generate data according to the flow chart shown in Figure 14. Given that the bridge had a length of 36.6 m, the fundamental frequency was obtained as 3.2 Hz, using Equation 1. However, per Table 1, a DLA of 0.25 was used for comparison based on the number of axles.

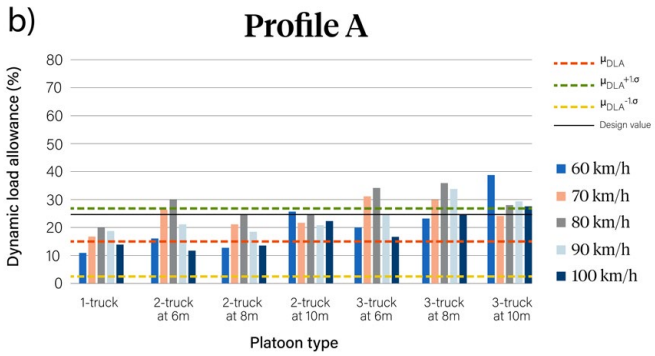
First, the DLA of single trucks on different surface roughness profiles was obtained and compared with the DLA proposed by CSA S6 for various speeds. It should be noted that in all cases, the calculated values were within the limits stipulated by the CSA S6 provisions [14]. As expected, surface roughness directly influenced the DLA values. However, this relationship was not linear, as shown in Figure 16a. For example, for profile A, the speed values directly influence the DLA from 60 km/h to 80 km/h, but this reverses with speed values of 80 km/h and above. Ling *et al.* [30] reported resonance for this span length at 80 km/h, which may explain this trend for the single truck moving on the bridge.

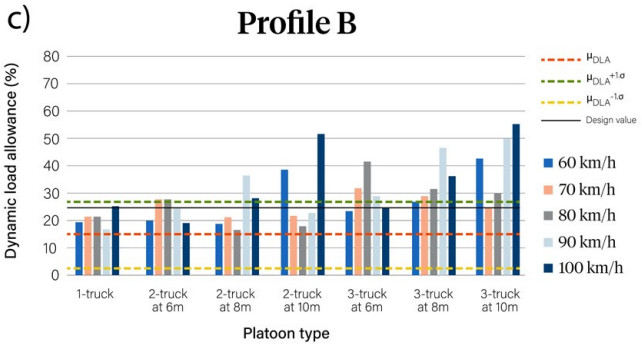
Next, a parametric study was performed for a total of 105 cases using the 3D finite element model generated in Abaqus to determine the effects of speed, spacing, number of trucks in platoons, and the level of pavement surface roughness profiles on the DLA. The value of 0.25 was compared with the DLA for 2-truck and 3-truck platoons and the three ISO 8608 roughness profiles, as shown in Figure 16b, 16c, and 16d. The DLA was less than 0.25 for 12 of 35 configurations with roughness profile A. The DLA was above 0.25 for 18 of 35 cases with roughness profile B, while the DLA was above 0.25 for 30 of 35 cases with roughness profile C. However, the latter is considered exceptionally large for bridges and would probably give rise to speed limitations and hence smaller DLA. Furthermore, the 0.25 DLA given in Table 1 for multiple axles is calibrated for a coefficient of variation of 80%, which accounts for the uncertainty on this value for bridges. Using a DLA of 0.25 and a bias coefficient of 0.6 given in Table C14.3 in CHBDC indicate a mean DLA (μ_{DLA}) of 0.15 but with a high COV of 80%. This results in a standard deviation (σ) of 12%. The DLA for the $\mu_{DLA} - 1.\sigma$ is 3% and the $\mu_{DLA} + 1.\sigma$ is 27%. This range envelopes the DLA range shown in Figure 16 a-c for for various single and platooning trucks configurations. In Equation 7, the DLA for a single truck was used as reference to evaluate the relative effect of platooning trucks on DLA.

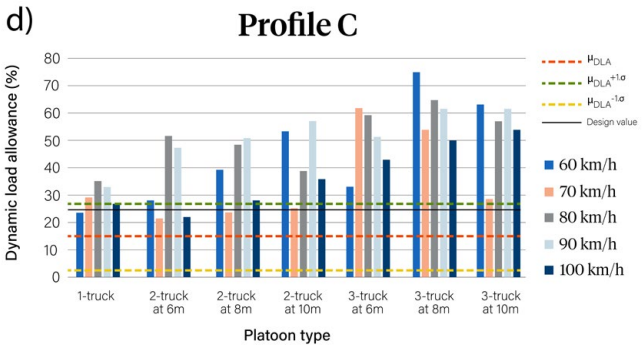
$$Relative\ difference = \frac{DLA_{platoon}}{DLA_{single\ truck}} \quad (7)$$

Figure 16: (a) DLA of single trucks modelled on different surface roughness profiles in comparison with CSA S6 provisions for speeds of 60 km/h, 70 km/h, 80 km/h, 90 km/h, and 100 km/h. DLA of different platoon truck configurations on ISO 8608 profile A (b), profile B (c), and profile C (d).







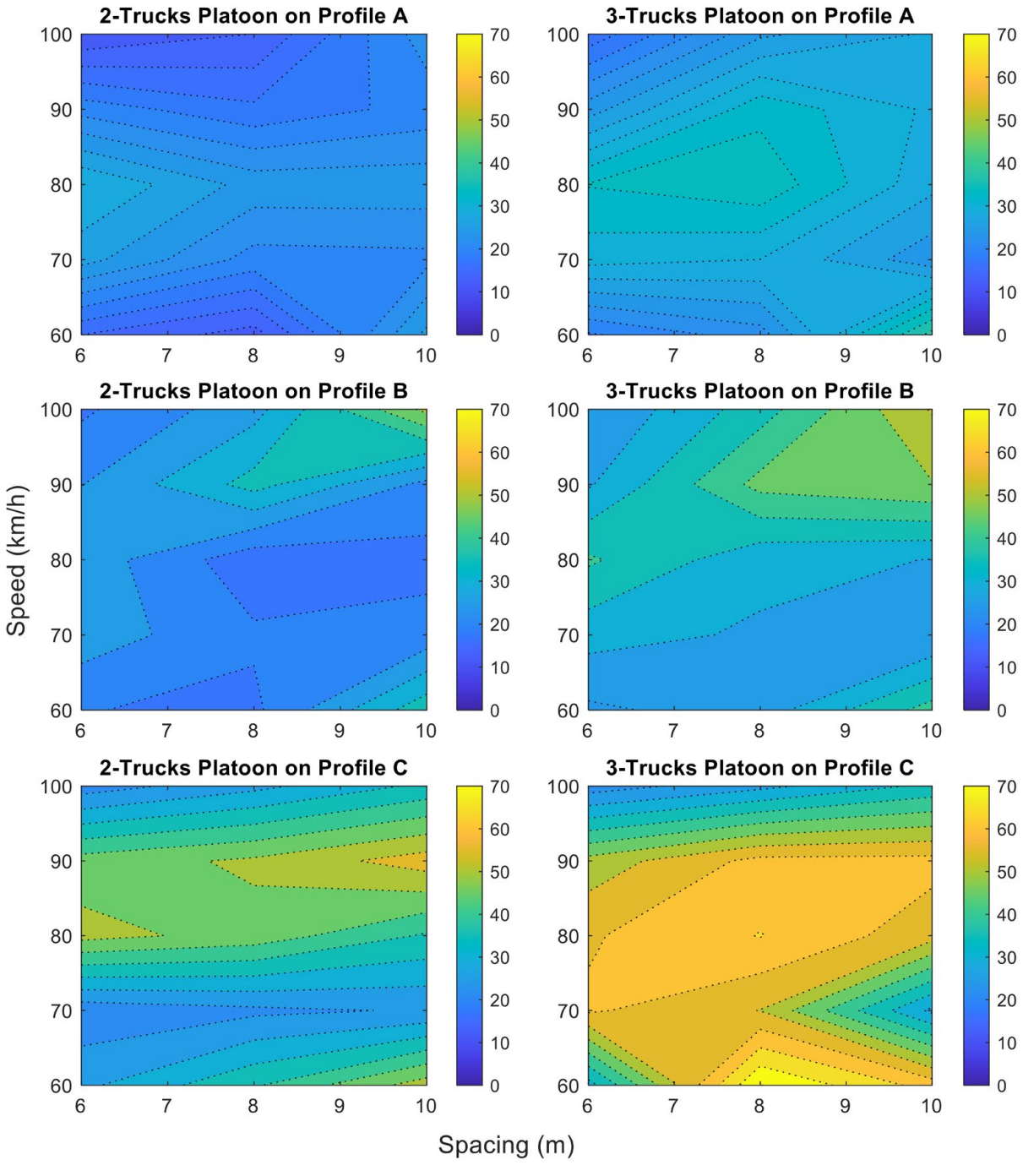


4.1 Effect of Speed and Inter-Truck Spacing

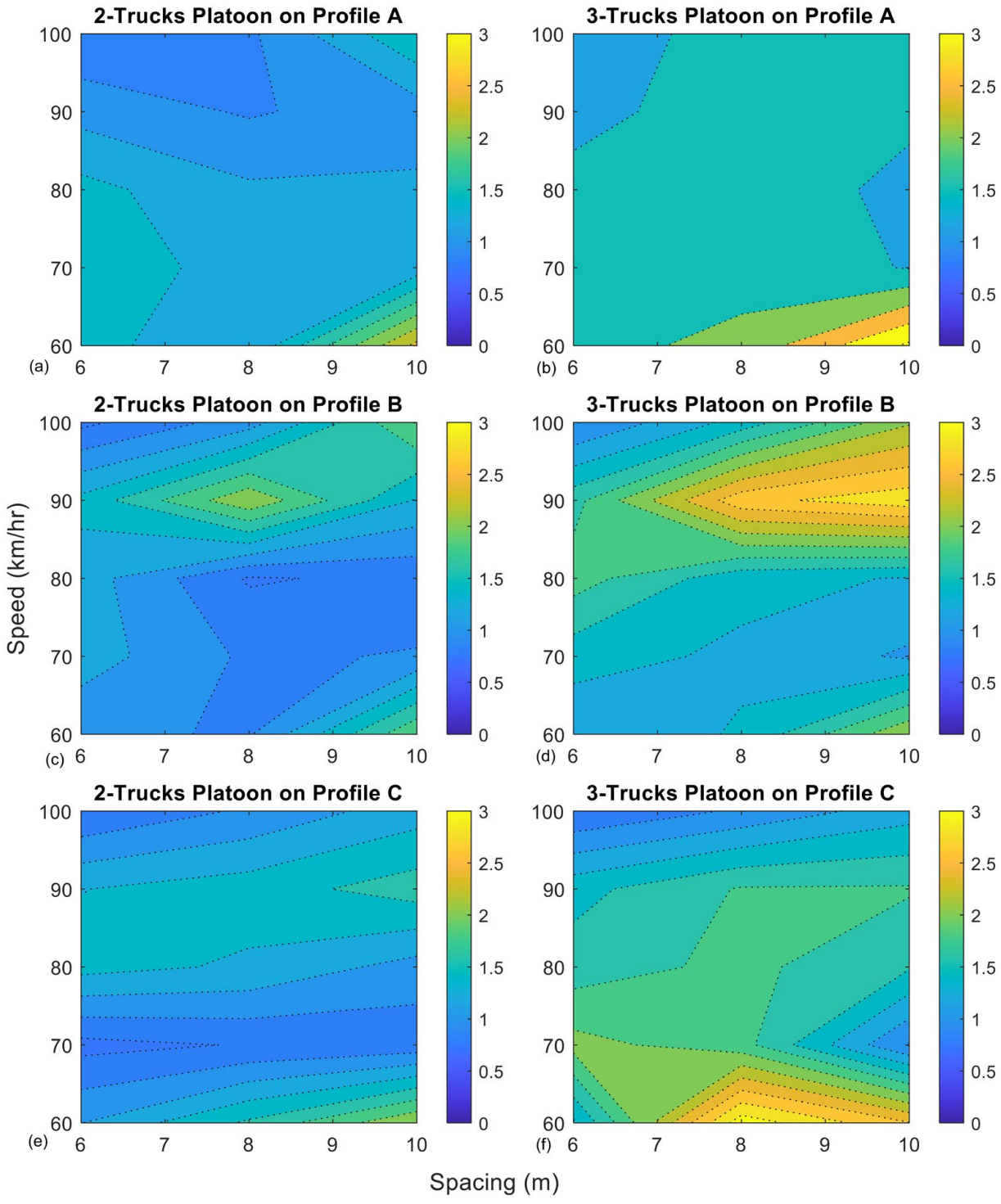
As indicated in Figure 14, speeds ranging from 60 to 100 km/h were considered for all platoon configurations and surface roughness profiles. The results indicate that the DLA does not always increase monotonically with increasing speed and decreasing inter-truck spacing. This behaviour is attributed to resonance effects that depend both on truck spacing and speed, and natural frequencies of the bridge [30]. The results also indicate that roughness of the surface profile is a contributing factor to the resonance of the bridge. In Figure 17a, the left column shows the DLA for the same platoon configurations for different surface profiles as a function of speed and spacing. Resonance occurred at different speeds and inter-truck spacings for the selected ranges for different roughness profiles. For example, the highest DLA for a 2-truck platoon due to resonance effects was observed at 80 km/h and 6 m inter-truck spacing on surface roughness profile A, while on profile B, it occurred at 100 km/h and 10 m inter-truck spacing, and on profile C, it occurred at 90 km/h and 10 m inter-truck spacing. The same can be observed for 3-truck platoon configurations on various profiles shown in the right column of Figure 17a. For the 3-truck platoon configurations, the maximum DLA due to resonance occurred at 60 km/h and 10 m inter-truck spacing on surface roughness profile A, while on profile B, it occurred at 100 km/h and 10 m inter-truck spacing, and on profile C, it occurred at 60 km/hr and 8 m inter-truck spacing.

The maximum DLA obtained for roughness profile C was for a 3-truck platoon with inter-truck spacing of 8 m and speed of 60 km/h (Figure 17a and 17b). In some instances, the DLA for platoons was smaller than that for a single truck, as shown in Figure 18b. This occurred for smooth profiles (A and B) for both 2-truck and 3-truck platoons but with no specific trend. These observations are consistent with previous results that show a decrease in DLA with an increase in the total static load in the absence of resonance [15]. Figure 17b also shows that, generally, lower DLAs relative to a single truck were observed for all the cases studied for ATPs moving at 100 km/h with 6 m inter-truck spacing. Similarly, inter-truck spacing seems to directly influence the DLA, as shown in most of the cases of 10 m inter-truck spacing (Figure 17). The upper limit of inter-truck spacing selected for this research was 10 m, as larger spacing can result in higher air-drag, which will diminish the fuel savings of platooning. These findings are consistent with Ling *et al.* [30], who also suggested that increasing inter-truck spacing may not be a solution to reduce the DLA from platooning loads. The number of trucks in a platoon also seems to have an influence on DLA, particularly for roughness profiles B and C. A higher number of trucks is not an issue from a static load perspective because the bridge span is smaller than the total length of the platoon. However, platoons that are longer than the length of the bridge generate dynamic loads over longer periods of time, which can result in higher DLA, as observed for 3-truck platoons and roughness profile C (Figure 17a and 17b). This issue could not be addressed in the research conducted for this report, but it should be further investigated.

Figure 17: (a) Effect of platoon speed and inter-truck spacing on DLA. The legend represents the DLA in percentage. (b) Ratio of DLA of different platooning configurations relative to DLA for a single truck as a function of speed and inter-truck spacing.



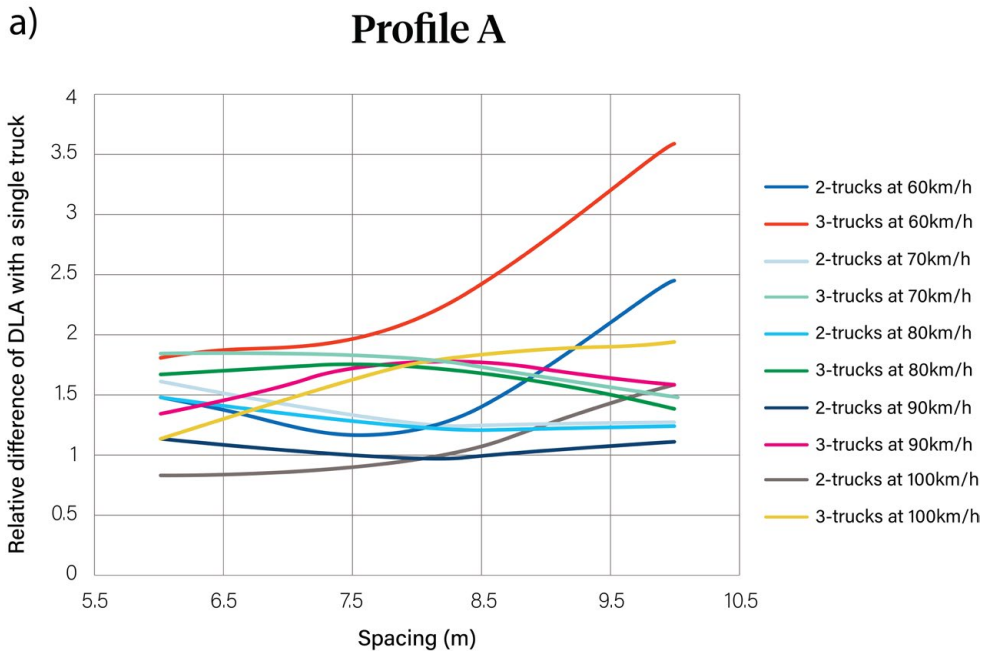
(a)


2-Trucks Platoon on Profile A
3-Trucks Platoon on Profile A
2-Trucks Platoon on Profile B
3-Trucks Platoon on Profile B
2-Trucks Platoon on Profile C
3-Trucks Platoon on Profile C
(a)
(b)
(c)
(d)
(e)
(f)
Speed (km/hr)
Spacing (m)
100
90
80
70
60
6
7
8
9
10
3
2.5
2
1.5
1
0.5
0

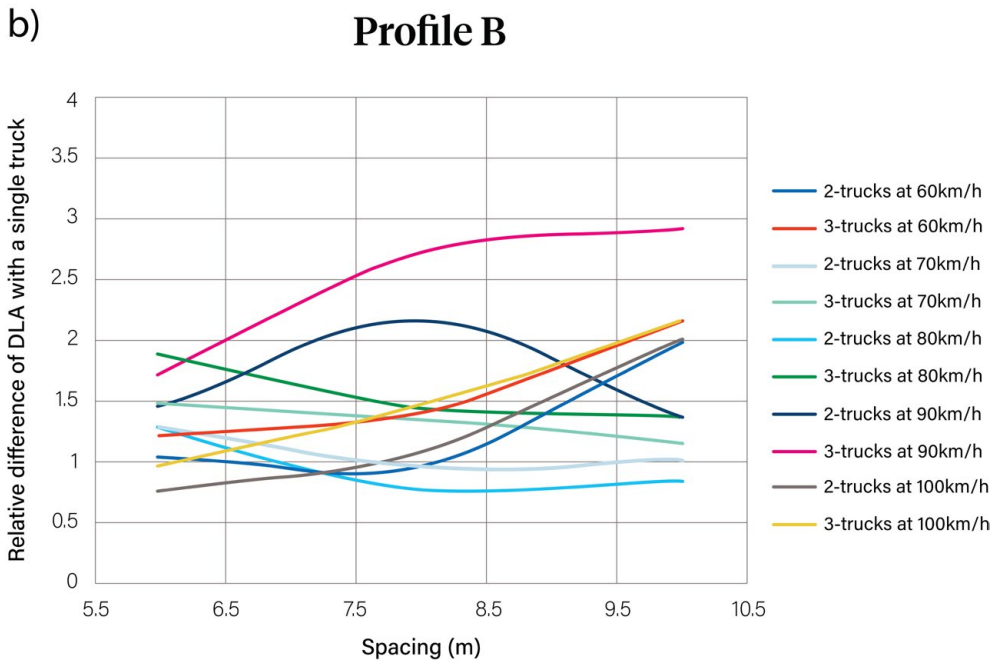
(b)

The effect of inter-truck spacing on DLA of platooning relative to a single truck for surface roughness profiles A, B, and C is illustrated in Figure 18. For profile A, only four of the ten platoon configurations (both the 2-truck and 3-truck platoons at 60 and 100 km/h) showed a direct relationship with inter-truck spacing in terms of a relative difference in DLA compared with a single truck (see Figure 18a). For profile B, in addition to the four configurations from profile A, 3-truck platoons at 90 km/h also showed an increasing trend in the relative difference in DLA compared with a single truck as a function of inter-truck spacing (see Figure 18b). For profile C, the trends in profiles A and B were not consistent for the 3-truck platoon configurations, but a direct relationship with inter-truck spacing in terms of a relative difference in DLA compared with a single truck was observed for 2-truck platoons at all speeds except 80 km/h (see Figure 18c). Consistent relationships are not always observed due to resonance effects between the dynamic platoon loads and the natural frequencies of the bridge. Smaller spacings could also result in more axles simultaneously on the bridge, which could exceed the loading limits of the bridge [53]. Karbasi *et al.* [54] demontrated that smaller headway spacings can increase the load demand above the capacity of the bridge at any speed.

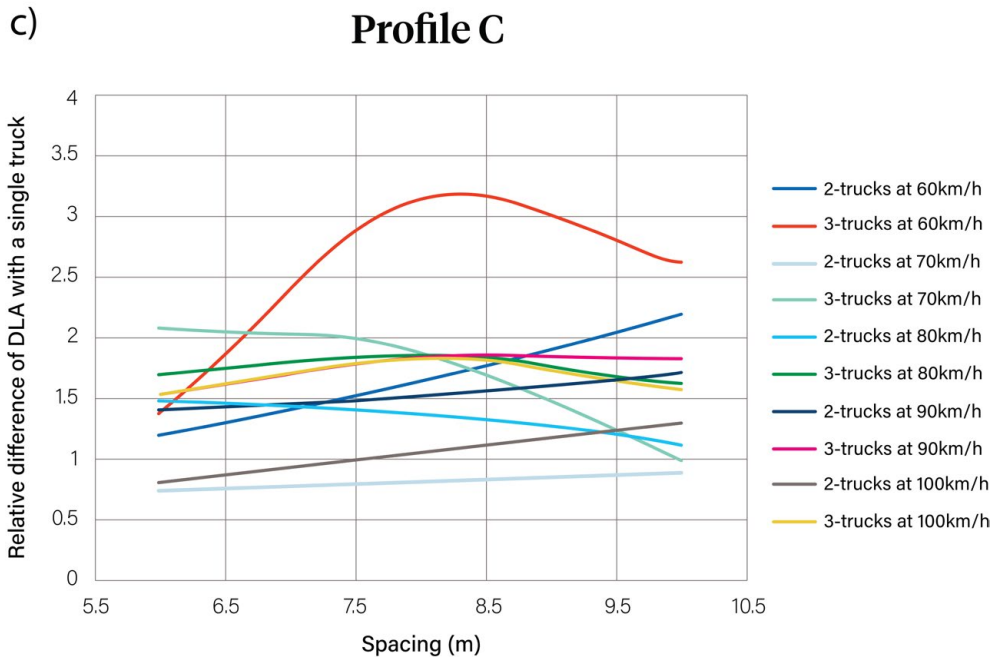
Figure 18: Effect of inter-truck spacing of platoon for each speed on the DLA for surface roughness profile A (a), profile B (b), and profile C (c).



b)


Profile B
Relative difference of DLA with a single truck
4
3.5
3
2.5
2
1.5
1
0.5
0
5.5
6.5
7.5
8.5
9.5
10.5
Spacing (m)
2-trucks at 60km/h
3-trucks at 60km/h
2-trucks at 70km/h
3-trucks at 70km/h
2-trucks at 80km/h
3-trucks at 80km/h
2-trucks at 90km/h
3-trucks at 90km/h
2-trucks at 100km/h
3-trucks at 100km/h

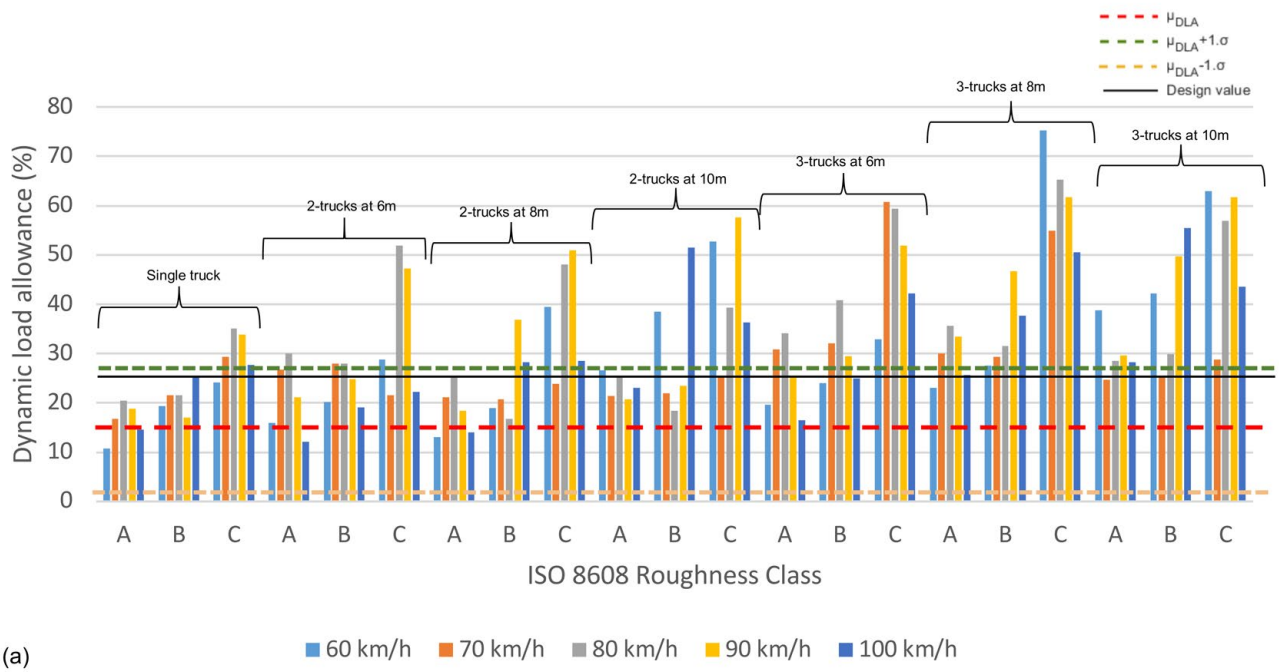
c)


Profile C
Relative difference of DLA with a single truck
4
3.5
3
2.5
2
1.5
1
0.5
0
5.5
6.5
7.5
8.5
9.5
10.5
Spacing (m)
2-trucks at 60km/h
3-trucks at 60km/h
2-trucks at 70km/h
3-trucks at 70km/h
2-trucks at 80km/h
3-trucks at 80km/h
2-trucks at 90km/h
3-trucks at 90km/h
2-trucks at 100km/h
3-trucks at 100km/h

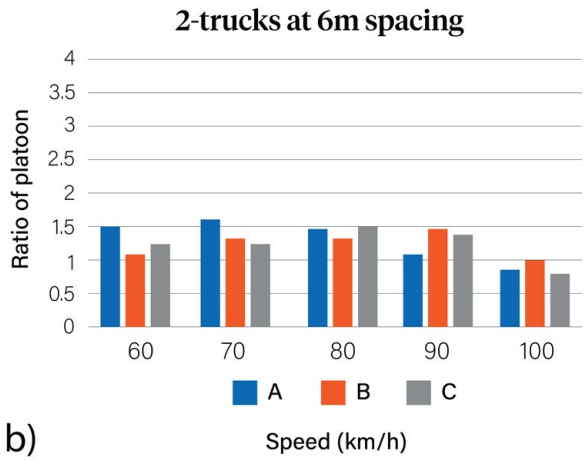
4.2 Effect of Pavement Surface Roughness

Pavement surface roughness is expected to directly increase the DLA, particularly when resonance occurs, as shown in Figure 16a and Figure 19a. The speed at which resonance occurs varies as a function of surface roughness. For example, resonance occurred at 80 km/h for roughness profile A for all platoon configurations except inter-truck spacings greater than 8 m for both 2-truck and 3-truck platoons. However, different platoon configurations have attained maximum DLAs due to resonance conditions at different surface roughness profiles. It is worth noting that the statistics given in Table 14.3C in CHBDC are generally consistent with the limits of mean and standard deviation given in Figure 19a for the various platooning arrangements and single trucks on relatively smoother surfaces (ISO Class A and Class B surface roughnesses). Figure 19(b) through 19(g) illustrates the ratio of platoon to single-truck DLA due to surface roughness for the various combinations of truck platoons investigated. For 2-truck platoons with inter-truck spacing of 6 m, the ratio was less than one at 100 km/h for all three surface roughness profiles. A similar trend was observed for almost half of the 2-truck configurations on profile B and a few configurations for profile A. There were only a few 3-truck configurations (6 m spacing at 100 km/h on profile B, and 10 m at 70 km/h on profiles B and C) where the DLA ratio was less than one.

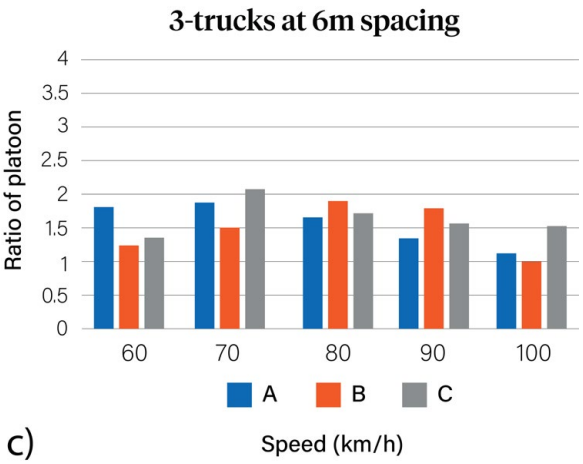
Figure 19: Effect of surface roughness profile on truck platoon DLA relative to that of a single truck.



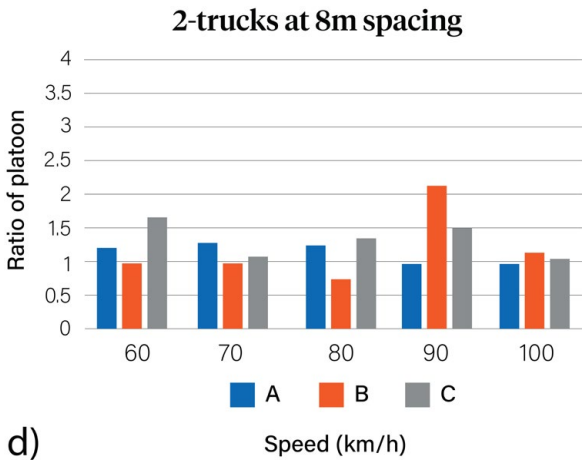
(a)


2-trucks at 6m spacing
Ratio of platoon
4
3.5
3
2.5
2
1.5
1
0.5
0
60
70
80
90
100
A
B
C
Speed (km/h)

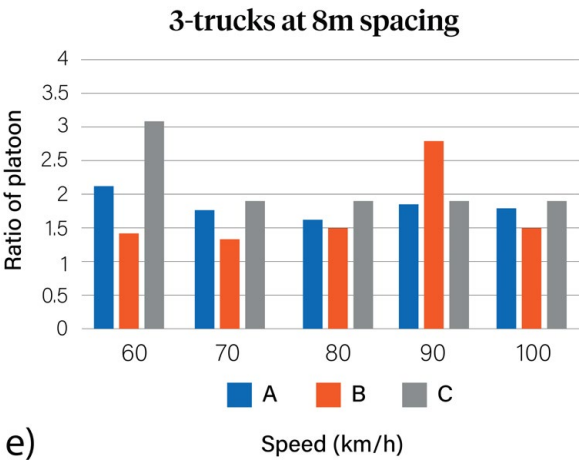
b)


3-trucks at 6m spacing
Ratio of platoon
4
3.5
3
2.5
2
1.5
1
0.5
0
60
70
80
90
100
A
B
C
Speed (km/h)

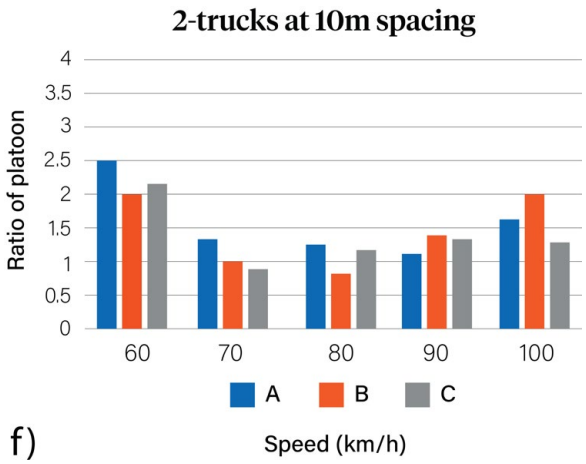
c)


2-trucks at 8m spacing
Ratio of platoon
4
3.5
3
2.5
2
1.5
1
0.5
0
60
70
80
90
100
A
B
C
Speed (km/h)

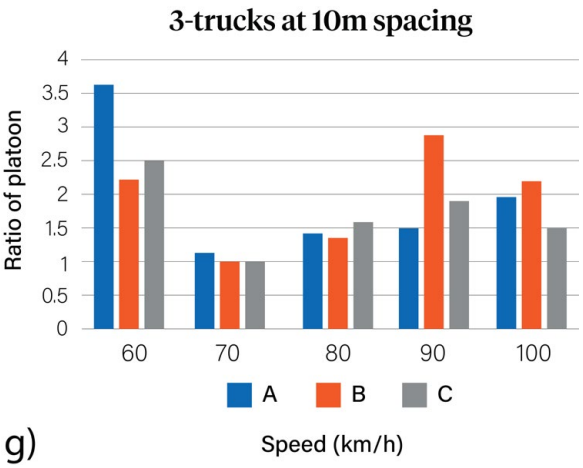
d)


3-trucks at 8m spacing
Ratio of platoon
4
3.5
3
2.5
2
1.5
1
0.5
0
60
70
80
90
100
A
B
C
Speed (km/h)

e)


2-trucks at 10m spacing
Ratio of platoon
4
3.5
3
2.5
2
1.5
1
0.5
0
60
70
80
90
100
A
B
C
Speed (km/h)

f)


3-trucks at 10m spacing
Ratio of platoon
4
3.5
3
2.5
2
1.5
1
0.5
0
60
70
80
90
100
A
B
C
Speed (km/h)

g)

5 Concluding Remarks

Autonomous truck platooning is under consideration as a cost saving strategy for the trucking industry. However, the capacity of existing bridges to accommodate this new technology has not been fully investigated.

The research conducted for this report aimed to understand the dynamic effects of ATPs on a single span steel girder concrete composite bridge. The parameters investigated were the number of trucks in a platoon (2–3), the inter-truck spacing (6–10 m), the speed (60–100 km/h), and the ISO 8608 road surface roughness profiles A, B, and C. A 3D finite element model of the bridge and surface roughness was developed in Abaqus. After analysis of the results, the main conclusions are:

a. Resonance, which is a function of surface roughness, platoon configuration, bridge characteristics, and ATP speed, is the governing factor in higher DLA for a given ATP configuration on the bridge.

b. For the ISO 8608 surface roughness profile A, most of the selected ATP configurations result in DLAs that are within the current limit specified in CSA S6 for the bridge considered in this report.

c. For ATPs with two to three trucks, the DLA is lower than the DLA for a single truck when the platoon configuration does not enter into resonance with the bridge.

d. An increase in the number of trucks in a platoon with large inter-truck spacing can correspond to resonance conditions that result in higher DLAs.

e. Higher speeds for 2-truck platoons with close spacing results in a marginal increase in DLA compared to that of a single truck on rougher surfaces, and can result in smaller DLAs than a single truck on smooth profiles.

f. A higher number of trucks in platoons at low speeds and over rough surfaces is conducive to resonance conditions and higher DLAs.

6 Recommendations for Future Work

Many issues were uncovered during the course of this research. However, the DLA for different bridge types and span lengths, and the statistical distribution of DLA could not be fully investigated. In order to develop comprehensive recommendations, the following topics for further research on autonomous truck platooning are suggested:

a. The effect of multiple types of vehicles on DLA should be investigated by simulating other vehicles moving alongside the platooning trucks.

b. More cases should be analyzed to generate a sufficiently large sample that can be used to perform statistical analyses for the calibration to the design code.

c. A number of trucks for platoon lengths greater than the length of the bridge (> 3) should be considered, as dynamic effects could be more severe due to the longer duration of dynamic loads.

d. Truck suspension system stiffness and damping should be further investigated given their influence on DLA.

e. Investigations should be expanded to include bridges with different span lengths and continuous bridges with multiple spans having different flexural frequencies.

f. Other bridge types (e.g., truss bridges and pre-stressed concrete girder bridges) should also be investigated.

g. Field studies should be performed on existing bridges as test cases.

References

[1] A. K. Bhoopalam, N. Agatz, and R. Zuidwijk, "Planning of truck platoons: A literature review and directions for future research," *Transportation research part B: methodological,* vol. 107, pp. 212–228, 2018, https://doi.org/10.1016/j.trb.2017.10.016.

[2] S. Tsugawa, S. Kato, and K. Aoki, "An automated truck platoon for energy saving," in *2011 IEEE/RSJ International Conference on Intelligent Robots and Systems,* 2011, pp. 4109–4114, https://doi.org/10.1109/IROS.2011.6094549.

[3] B. McAuliffe, M. Lammert, X.-Y. Lu, S. Shladover, M.-D. Surcel, and A. Kailas, "Influences on energy savings of heavy trucks using cooperative adaptive cruise control," SAE International, Warrendale, PA, United States, SAE Technical Paper 0148-7191, 2018. [Online]. Available: https://doi.org/10.4271/2018-01-1181

[4] L. Zhang, T. Zhang, K. Peng, X. Zhao, and Z. Xu, "Can autonomous vehicles save fuel? Findings from field experiments," *Journal of Advanced Transportation,* 2022, Art. No. 2631692, https://doi.org/10.1155/2022/2631692.

[5] Bureau of Transportation Statistics. "2017 CFS preliminary data." [Online]. Available: https://www.bts.gov/surveys/commodity-flow-survey/2017-cfs-preliminary-data

[6] B. van Arem, C. J. van Driel, and R. Visser, "The impact of cooperative adaptive cruise control on traffic-flow characteristics," *IEEE Transactions on Intelligent Transportation Systems,* vol. 7, no. 4, pp. 429–436, 2006, https://doi.org/10.1109/TITS.2006.884615.

[7] J. Lioris, R. Pedarsani, F. Y. Tascikaraoglu, and P. Varaiya, "Platoons of connected vehicles can double throughput in urban roads," *Transportation Research Part C: Emerging Technologies,* vol. 77, pp. 292–305, 2017, https://doi.org/10.1016/j.trc.2017.01.023.

[8] I. Alsghan, M. V. Chitturi, and D. A. Noyce, "Road sign occlusion under truck platooning," *Journal of Transportation Engineering, Part A: Systems,* vol. 147, no. 9, 2021, Art. no. 04021045, https://doi.org/10.1061/JTEPBS.0000553.

[9] S. Lee, C. Oh, and G. Lee, "Impact of automated truck platooning on the performance of freeway mixed traffic flow," *Journal of Advanced Transportation,* 2021, Art. no. 8888930, https://doi.org/10.1155/2021/8888930.

[10] M. M. Rana, "Effect of autonomous vehicles on pavement distress and road safety and pavement distress optimization," M.S. thesis, Faculty of Engineering and Applied Science, Memorial University of Newfoundland, St. John's, NL, Canada, 2021. [Online]. Available: https://doi.org/10.48336/SCD4-2A58

[11] M. Scott, M. Zhu, P. Oleson, T. Schumacher, and A. Unnikrishnan, "Impact of truck platooning on loading of bridges in Oregon," Oregon Department of Transportation, Research Section, Salem, OR, United States, Rep. no. FHWA-OR-RD-24-09, 2024. [Online]. Available: https://www.oregon.gov/odot/Programs/ResearchDocuments/SPR848_ImpactOfTruckPlatooning.pdf

[12] S. Sajid, L. Chouinard, F. Legeron, T. Ude, E. He, and J. Ajrab, "Reliability analysis of bridges for autonomous truck platoons," *Transportation Research Record,* vol. 2677, no. 1, pp. 1071–1081, 2023, https://doi.org/10.1177/03611981221103235.

[13] *AASHTO LRFD Bridge Design Specifications,* 9th Edition, American Association of State Highway and Transportation Officials, Washington, DC, United States, 2020. [Online]. Available: https://store.transportation.org/Item/CollectionDetail?ID=202

[14] *Canadian Highway Bridge Design Code,* CSA S6:19, Canadian Standards Association, Toronto, ON, Canada, 2019. [Online]. Available: https://www.csagroup.org/store/product/2701232/

[15] A. S. Nowak, "Calibration of LRFD bridge design code," National Cooperative Highway Research Program, Transportation Research Board, Washington, DC, United States, pp. 9–28, Rep. 368, 1999. [Online]. Available: http://onlinepubs.trb.org/Onlinepubs/nchrp/nchrp_rpt_368.pdf

[16] M. Lutomirska, "Live load models for long span bridges," Ph.D. dissertation, Dept. Civil and Environmental Engineering, University of Nebraska, Lincoln, NE, United States, 2009. [Online]. Available: https://digitalcommons.unl.edu/civilengdiss/1

[17] E.-S. Hwang and A. S. Nowak, "Simulation of dynamic load for bridges," Journal of Structural Engineering, vol. 117, no. 5, pp. 1413–1434, 1991, https://doi.org/10.1061/(ASCE)0733-9445(1991)117:5(1413).

[18] S. M. Sayed, H. N. Sunna, and P. R. Moore, "Truck platooning impact on bridge preservation," *Journal of Performance of Constructed Facilities,* vol. 34, no. 3, 2020, Art. no. 04020029, https://doi.org/10.1061/(ASCE)CF.1943-5509.0001423.

[19] M. T. Yarnold and J. S. Weidner, "Truck platoon impacts on steel girder bridges," *Journal of Bridge Engineering,* vol. 24, no. 7, 2019, Art. no. 06019003, https://doi.org/10.1061/(ASCE)BE.1943-5592.0001431.

[20] R. Tohme and M. Yarnold, "Steel bridge load rating impacts owing to autonomous truck platoons," *Transportation Research Record,* vol. 2674, no. 2, pp. 57–67, 2020, https://doi.org/10.1177/0361198120902435.

[21] T. Couto Braguim, P. Lou, and H. Nassif, "Truck platooning to minimize load-induced fatigue in steel girder bridges," *Transportation Research Record,* vol. 2675, no. 4, pp. 146–154, 2020, https://doi.org/10.1177/0361198120973657.

[22] T. Ling, L. Deng, W. He, H. Wu, and J. Deng, "Load effect of automated truck platooning on highway bridges and loading strategy," *Sensors,* vol. 22, no. 20, 2022, Art. no. 7704, https://doi.org/10.3390/s22207704.

[23] *Manual for Bridge Evaluation,* 3rd Edition, American Association of State Highway and Transportation Officials, Washington, DC, United States, 2018. [Online]. Available: https://store.transportation.org/Item/PublicationDetail?ID=4135

[24] M. T. Elshazli, A. Ibrahim, and A. Abdel-Rahim, "Truck platooning impact on existing bridges' load ratings," *Structures,* vol. 51, 2023, pp. 1706–1721, https://doi.org/10.1016/j.istruc.2023.03.131.

[25] M. Elshazli, A. Ibrahim, and A. Abdel-Rahim, "Impact of autonomous and connected truck platoons in the Pacific Northwest on transportation infrastructure," Pacific Northwest Transportation Consortium, Seattle, WA, United States, Rep. no. 2021-S-UI-2, 2022. [Online]. Available: https://rosap.ntl.bts.gov/view/dot/64114

[26] N. P. Thulaseedharan and M. T. Yarnold, "Prioritization of Texas prestressed concrete bridges for future truck platoon loading," *Bridge Structures,* vol. 16, no. 4, pp. 155–167, 2020, http://dx.doi.org/10.3233/BRS-210181.

[27] W. Wassef, "Truck platooning impacts on bridges: Phase I – Structural safety," United States Department of Transportation, Federal Highway Administration, Washington, DC, United States, Rep. no. FHWA-HIF-21-043, Jul. 2021. [Online]. Available: https://www.fhwa.dot.gov/bridge/loadrating/pubs/hif21043.pdf

[28] B. Yang, J. S. Steelman, J. A. Puckett, and D. G. Linzell, "Safe platooning headways on girder bridges," *Transportation Research Record,* 2021, https://doi.org/10.1177/03611981211036379.

[29] J. S. Steelman, J. A. Puckett, D. G. Linzell, and B. Yang, "Truck platooning effects on girder bridges," Nebraska Department of Transportation, Lincoln, NE, United States, Rep. no. SPR-1(20) M030, Jan. 2021. [Online]. Available: https://dot.nebraska.gov/media/vvalloir/spr-1-20-m030-truck-platooning-effects-on-girder-bridges-final-report.pdf

[30] T. Ling, R. Cao, L. Deng, W. He, X. Wu, and W. Zhong, "Dynamic impact of automated truck platooning on highway bridges," *Engineering Structures,* vol. 262, 2022, Art. no. 114326, https://doi.org/10.1016/j.engstruct.2022.114326.

[31] T. Ling, L. Deng, W. He, R. Cao, and W. Zhong, "Determination of dynamic amplification factors for small- and medium-span highway bridges considering the effect of automated truck platooning loads," *Mechanical Systems and Signal Processing,* vol. 204, 2023, Art. no. 110812, https://doi.org/10.1016/j.ymssp.2023.110812.

[32] G. P. Tilly, "Dynamic behaviour of concrete structures: Report of the RILEM 65-MDB Committee," *Materials and Structures,* vol. 19, p. 460, 1986, https://doi.org/10.1007/BF02472155.

[33] P. Paultre, O. Chaallal, and J. Proulx, "Bridge dynamics and dynamic amplification factors—a review of analytical and experimental findings," Canadian Journal of Civil Engineering, vol. 19, no. 2, pp. 260–278, 1992, https://doi.org/10.1139/l92-032.

[34] *Standard Specifications for Highway Bridges,* American Association of State Highway and Transportation Officials, Washington DC, United States, 2002. [Online]. Available: https://store.transportation.org/Item/CollectionDetail?ID=15

[35] *Eurocode 1. Actions on Structures – Part 2: Traffic Loads on Bridges,* BS EN 1991-2, British Standards Institution, London, United Kingdom, 2003. [Online]. Available: https://knowledge.bsigroup.com/products/eurocode-1-actions-on-structures-traffic-loads-on-bridges

[36] L. Deng, Y. Yu, Q. Zou, and C. S. Cai, "State-of-the-art review of dynamic impact factors of highway bridges," *Journal of Bridge Engineering,* vol. 20, no. 5, 2015, Art. no. 04014080, https://doi.org/10.1061/(ASCE)BE.1943-5592.0000672.

[37] L. Gao, "Reliability-based evaluation of bridges live load carrying capacity in the United States," Public Works Research Institute, Ibaraki, Japan, 2012. [Online]. Available: https://www.pwri.go.jp/eng/ujnr/tc/g/pdf/28/28-3-2_Gao.pdf

[38] Y.-B. Yang and J.-D. Yau, "Vehicle-bridge interaction element for dynamic analysis," *Journal of Structural Engineering,* vol. 123, no. 11, pp. 1512–1518, 1997, https://doi.org/10.1061/(ASCE)0733-9445(1997)123:11(1512).

[39] K. Chang, F. B. Wu, and Y. B. Yang, "Disk model for wheels moving over highway bridges with rough surfaces," *Journal of Sound and Vibration,* vol. 330, no. 20, pp. 4930–4944, 2011, https://doi.org/10.1016/j.jsv.2011.05.002.

[40] A. Ben Afia, C.-D. Annan, and P. Dey, "Dynamic behavior of aluminum deck-on-steel girders bridges under vehicular loads considering the effect of road roughness," in *IABSE Congress: Structural Engineering for Future Societal Needs,* Ghent, Belgium, Sep. 22–24, 2021, pp. 1623–1632, https://doi.org/10.2749/ghent.2021.1623.

[41] W. Gao, N. Zhang, and J. Dai, "A stochastic quarter-car model for dynamic analysis of vehicles with uncertain parameters," *Vehicle System Dynamics,* vol. 46, no. 12, pp. 1159–1169, 2008, https://doi.org/10.1080/00423110701884575.

[42] F. Tyan, Y.-F. Hong, S.-H. Tu, and W. S. Jeng, "Generation of random road profiles," *Journal of Advanced Engineering,* vol. 4, no. 2, pp. 151–156, 2009, https://doi.org/10.29948/JAE.200904.0009.

[43] T. Lenkutis, A. Čerškus, N. Šešok, A. Dzedzickis, and V. Bučinskas, "Road surface profile synthesis: Assessment of suitability for simulation," *Symmetry,* vol. 13, no. 1, 2020, Art. no. 68, https://doi.org/10.3390/sym13010068.

[44] P. Andren, "Power spectral density approximations of longitudinal road profiles," *International Journal of Vehicle Design,* vol. 40, no. 1/2/3, pp. 2–14, 2006, https://doi.org/10.1504/IJVD.2006.008450.

[45] M. Agostinacchio, D. Ciampa, and S. Olita, "The vibrations induced by surface irregularities in road pavements–a Matlab® approach," *European Transport Research Review,* vol. 6, no. 3, pp. 267–275, 2014, https://doi.org/10.1007/s12544-013-0127-8.

[46] *Mechanical Vibration — Road Surface Profiles — Reporting of Measured Data,* ISO 8608, International Organization for Standardization, Geneva, Switzerland, 2016. [Online]. Available: https://www.iso.org/standard/71202.html

[47] P. Múčka, "International Roughness Index specifications around the world," *Road Materials and Pavement Design,* vol. 18, no. 4, pp. 929–965, 2017, https://doi.org/10.1080/14680629.2016.1197144.

[48] G. Loprencipe and P. Zoccali, "Use of generated artificial road profiles in road roughness evaluation," *Journal of Modern Transportation,* vol. 25, pp. 24–33, 2017, https://doi.org/10.1007/s40534-017-0122-1.

[49] N. K. Harris, E. J. O'Brien, and A. González, "Reduction of bridge dynamic amplification through adjustment of vehicle suspension damping," *Journal of Sound and Vibration,* vol. 302, no. 3, pp. 471–485, 2007, https://doi.org/10.1016/j.jsv.2006.11.020.

[50] M. F. Green, D. Cebon, and D. J. Cole, "Effects of vehicle suspension design on dynamics of highway bridges," *Journal of Structural Engineering,* vol. 121, no. 2, pp. 272–282, 1995, https://doi.org/10.1061/(ASCE)0733-9445(1995)121:2(272).

[51] L. Deng and C. S. Cai, "Development of dynamic impact factor for performance evaluation of existing multi-girder concrete bridges," *Engineering Structures,* vol. 32, no. 1, pp. 21–31, 2010, https://doi.org/10.1016/j.engstruct.2009.08.013.

[52] Y. Lim and S. Ha, "RufGen: A plug-in for rough surface generation in Abaqus/CAE," *SoftwareX,* vol. 22, 2023, Art. no. 101380, https://doi.org/10.1016/j.softx.2023.101380.

[53] J. S. Steelman, J. A. Puckett, D. G. Linzell, and B. Yang, "Truck platooning effects on girder bridges: Phase II – Service," Nebraska Department of Transportation, Lincoln, NE, United States, Rep. no. SPR-FY22(011), 2023. [Online]. Available: https://dot.nebraska.gov/media/0ese55i1/spr-fy22-011-final-report-ver2.pdf

[54] A. H. Karbasi, M. Xu, H. He, S. Budisa, H. Yang, and C. Yang, "The Impact of Truck Platooning on Traffic Flow Considering Bridge Safety Index," in *2023 IEEE 26th International Conference on Intelligent Transportation Systems (ITSC),* Bilbao, Spain, Sep. 24–28, 2023, pp. 2016–2022, https://doi.org/10.1109/ITSC57777.2023.10421929.

[55] British Standards Institution (BSI). *Steel, concrete, and composite bridges. Part 2: Specification for loads.* BS 5400-2, London. 2006.

CSA Group Research

In order to encourage the use of consensus-based standards solutions to promote safety and encourage innovation, CSA Group supports and conducts research in areas that address new or emerging industries, as well as topics and issues that impact a broad base of current and potential stakeholders. The output of our research programs will support the development of future standards solutions, provide interim guidance to industries on the development and adoption of new technologies, and help to demonstrate our on-going commitment to building a better, safer, more sustainable world.

CSA GROUP™

© 2024 Canadian Standards Association. All Rights Reserved.